RESERVOIR CHARACTERIZATION OF SELECTED DISTAL FRIO FORMATION FIELDS OF TEXAS

By W. E. Galloway and R. A. Morton

Final Report

Prepared for the U.S. Department of Interior
Minerals Management Service
Cooperative Agreement No. 14-12-0001-30316

Bureau of Economic Geology
W. L. Fisher, Director
The University of Texas at Austin

April 1988

QAe7549

CONTENTS

FIGURES

ABSTRACT

Thick, aggradational sequences of shelf and distal shoreface sandstones are prolific hydrocarbon reservoirs in the deep, downdip part of the Frio Formation fronting the Greta/Caranchahua shorezone system. Near Corpus Christi, Texas, geopressured shelf reservoirs have produced more than 190 bcf of gas just in the Corpus Channel and Encinal Channel fields; within these fields, two thinly bedded shelf-sandstone units (K2 and K8 reservoirs) have produced 26 and 38 bcf of gas respectively.

Cross sections and maps show that shelf sandstones extend basinward from the distal shoreface toes of barrier-island and beach-ridge sandstone bodies. Shelf sequences are typically upward-coarsening, although upward-fining and heterogeneous sequences also occur. Conventional cores reveal that shelf sequences consist of bioturbated muddy sandstone and sandy mudstone thinly interbedded with planar laminated, sparsely burrowed, and occasionally low-angle cross-laminated or ripple-laminated fine to very fine sandstone. Associated burrow-homogenized siltstone to very fine sandstone sequences are from 1.5 to 6 m (5 to 20 ft) thick. Scattered thin zones contain locally derived mudstone clasts, macerated plant fragments, or shell debris. Individual shelf sandstone bodies commonly exceed 30 m (100 ft) in thickness, particularly where expanded on the downthrown side of major growth faults. In plan view, shelf sandstones are irregular sheets covering areas of several hundreds of square kilometers. Sandstone percent maps reveal subparallel, discontinuous, strike-oriented buildups lying seaward of the contemporary shoreface sandstone unit. These shore-parallel belts are typically interconnected and attached to the shoreface sand body by one or more dip-oriented channel-like axes.

The geometry and internal features of the shelf sandstones document their deposition and longshore reworking by storm processes. Focused bottom return flow swept sand from the shoreface onto the inner shelf where it was distributed alongshore by wind-forced geostrophic currents. Between the infrequent, high-energy storm events, a diverse shelf infauna reworked the sediments. Although a turbidity current origin has commonly been suggested for similar shelf sequences in the Frio and other stratigraphic units, the geometry, trend, setting and internal sedimentary structures are incompatible with this depositional process.

Reservoir characteristics of Frio shelf sandstones are controlled by original pore properties inherited from the depositional environment and by subsequent diagenetic processes. The reservoirs are composed of moderate to well sorted fine to very fine quartzose lithic arkoses that contain abundant glauconite pellets. Volcanic rock fragments dominate the lithic component, although some mudstone fragments are present in all samples. Cements are mainly quartz and feldspar overgrowths with minor amounts of sparry calcite, kaolinite, and clay coats; porosity also is reduced by deformed rock

fragments. Optimum reservoir porosities range from 16 to 30 percent and average about 23 percent. Permeabilities for the same intervals range from 0 to 1200 md; however, such extremes are rare and values of tens to hundreds of millidarcies are most common. Reservoir quality improves at depth by dissolution of feldspar grains. This secondary porosity accounts for nearly half of the total porosity.

Subregional megascopic heterogenieties occur as alternating zones of higher and lower permeability oriented parallel to depositional strike and spaced a few kilometers apart. Within a field, lateral and vertical variations in pore properties primarily depend on facies sequences and degree of burrowing. High and intermediate permeabilities coincide with ripple cross laminations and plane parallel laminations respectively, whereas low permeabilities coincide with bioturbated strata.

INTRODUCTION

Like the Holocene depositional history of the northwest margin of the Gulf of Mexico, the Cenozoic Era was dominated by progradation of major deltaic complexes and flanking wave-dominated shore-zone systems. During active progradation of the clastic wedges, marine shelves were comparatively narrow and generally restricted to positions between major deltaic headlands (Jackson and Galloway 1984). During and following major transgressive events that punctuate the history of Cenozoic offlap, shallow to deep-water shelf environments spread extensively across flooded paralic and coastal plain platforms. Thus two varieties of shelf regimes are found repeated throughout the stratigraphic record of the Gulf of Mexico.

Today, as during the Cenozoic Era, intermittent storms provide the energy capable of transporting sand from the shoreface prism and sweeping it onto the adjacent shelf (Hayes 1967; Morton 1981). The low-energy fairweather conditions in the Gulf of Mexico (characteristic of Mediterranean type basins) generally were incapable of extensive bedload transport onto the shelf; therefore, the shelf sequences are dominately muddy. However, locally significant shelf sand facies do exist. In this paper, we describe sedimentological attributes and reservoir properties of a relatively sandy shelf depositional system and review its hydrocarbon production characteristics.

FRIO SHELF SANDSTONE FACIES OF THE CORPUS CHRISTI BAY AREA

The Oligocene Frio Formation of the Middle Texas Coastal Plain, extending from the vicinity of Corpus Christi northeastward to the area of Brazoria County, records deposition along a major wave-dominated coastline (Galloway et al. 1982). This sand-rich shore-zone depositional system, which was named the Greta/Carancahua barrier/strandplain, lies between the Norias delta system (Fig. 1) and the Houston delta system (not shown). Deep drilling for gas and condensate reservoirs has revealed that thick, locally sandy, deposits of a narrow shelf lie basinward of the Greta/Carancahua barrier/strandplain system (Galloway 1986b). Laterally extensive, shoreface-attached sandstone units are particularly well developed in the vicinity of Corpus Christi Bay, where the Greta barrier system grades into deposits of the Norias deltaic depocenter (Fig. 1). At this paleogeographic location, packets of interbedded sand and mudstone occur within thick, growth-fault expanded sections of marine shelf mudstones at the base of the offlapping Frio genetic depositional sequence (Fig. 2). The sandy packets can be correlated updip across growth faults into equivalent massive shoreface and barrier-core sandstones of the progradational lower Frio shore zone. Downdip, sandy packets grade into massive mudstones of the lower Frio continental margin facies sequence. High growth ratios across faults (thickness of unit on downthrown block/thickness of unit on upthrown block) indicate that deposition of the delta-flank barriers and their equivalent sandstone packets occurred near the structurally active prograding continental margin (Winker 1982; Jackson and Galloway 1984).

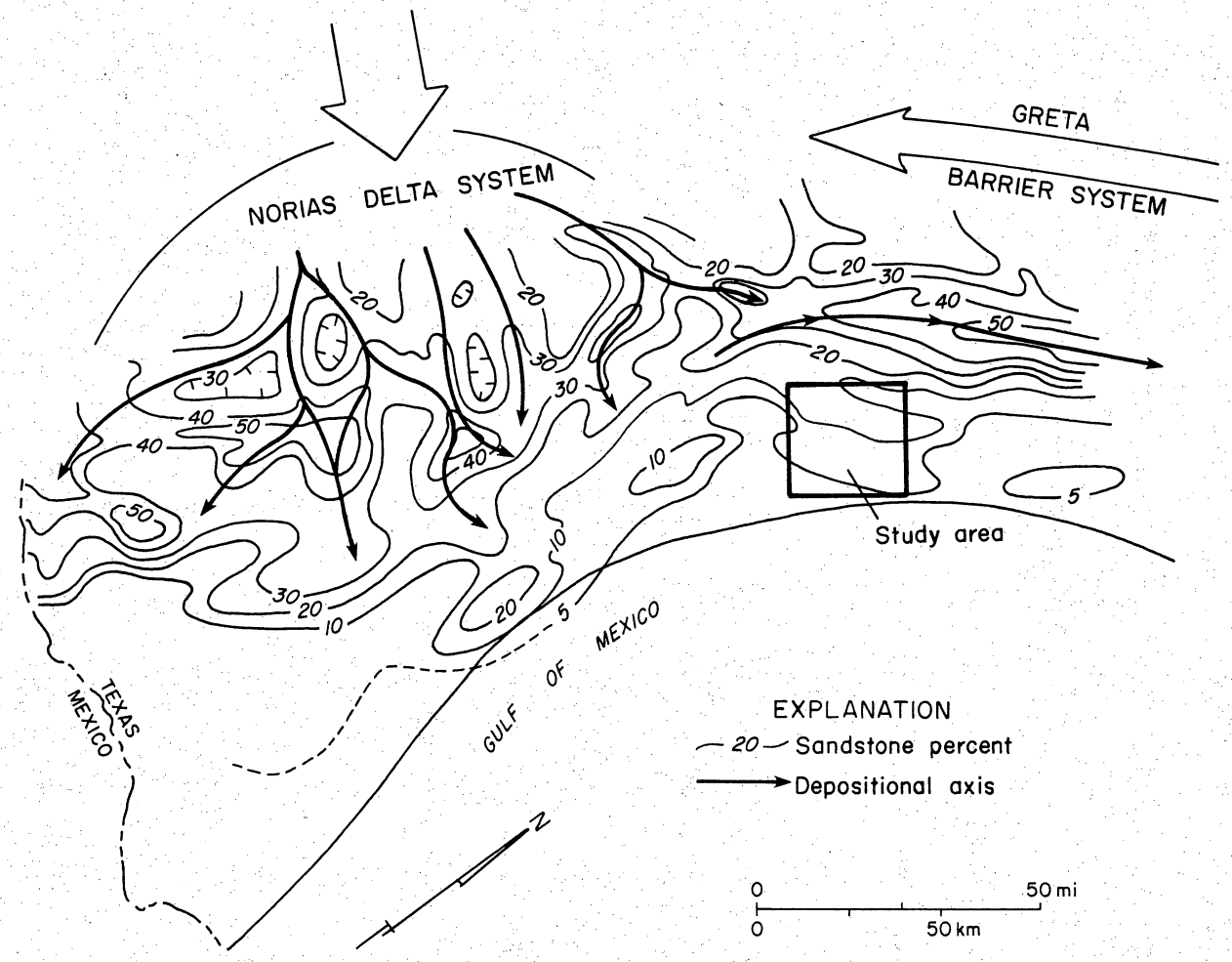

Figure 1. Depositional systems and sandstone percentage of the lower Frio Formation. Location of the study area is shown by the box. From Galloway (1986b).

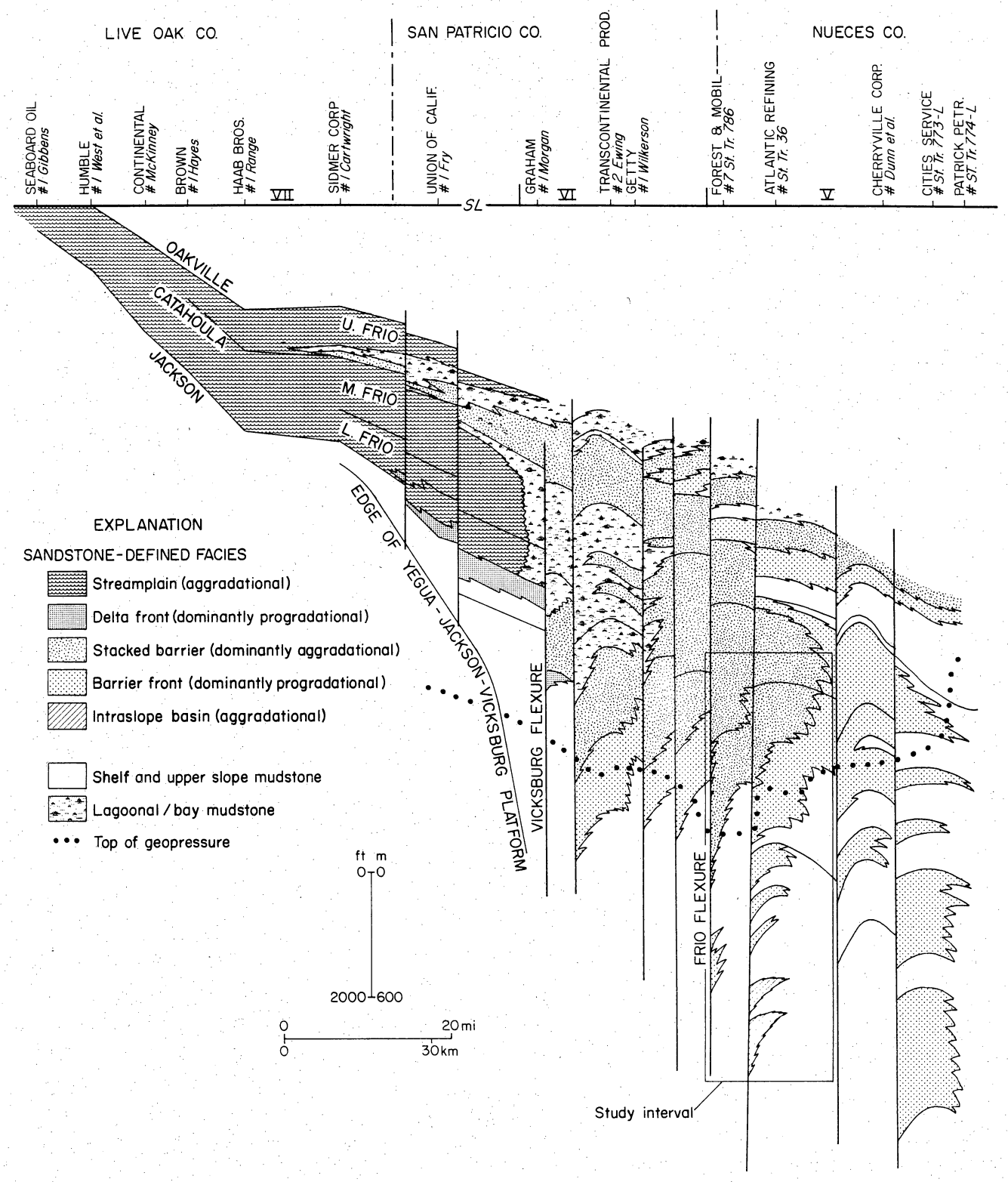

Figure 2. Regional dip cross section of the Greta/Carancahua barrier/strandplain system in the Corpus Christi area. The stratigraphic location of the studied shorezone-to-shelf facies sequences is outlined by the box. The facies is in the lower, progradational part of the Greta barrier complex. From Galloway (1986b).

An area extending from central Corpus Christi Bay through the southern tip of Aransas County provided a natural laboratory to examine the sedimentologic and reservoir characteristics of these distal sands of the Frio barrier/strandplain system. Several gas and condensate fields that produce from the deep Frio sandstones lie within the area; consequently well control is relatively abundant and several convential cores were available for study (Fig. 3). The area encompasses parts of two fault blocks. The updip (northwest) limit parallels a major growth fault that shows little displacement of the lower Frio sandstones. The downdip (southeast) limit is a major growth fault that displaces the lower Frio sandstone section below current limits of deep drilling. A major growth fault bisects the study area providing the opportunity to examine the relationship of depositional patterns to contemporaneous faulting and differential subsidence.

The following description of sand-body geometries, facies relationships, and internal features is based on a network of log cross sections, detailed lithofacies maps of correlative, thin genetic units (called map units), and examination of more than 100 m (350 ft) of continuous core.

Three-Dimensional Facies Relationships

Electrical log cross sections (Fig. 4) illustrate the facies tract developed basinward from typical stacked barrier core and associated proximal shoreface sandstone bodies. Updip (northwest), the map units are characterized by blocky to upward-coarsening sand bodies that are typically 10 to 15 m (30 to 50 ft) thick. Thickness, log profiles, and mapped sand-distribution patterns are typical of progradational barriers of the Frio Greta/Carancahua system (Galloway et al. 1982, Galloway 1986b). In the mid-dip fault block (wells 5 through 6, Fig. 4) thicker, but increasingly interbedded (serrate log pattern) sandstone packets are recognized, and bounding mudstone units are better defined. Across the major growth fault that bisects the study area, the relatively compressed updip sections expand more than five-fold. Rapid subsidence led to nearly complete storage of introduced sediment, and individual depositional packets can be differentiated and correlated downdip to the limits of well control (wells 7 through 24, Fig. 4). In both intervals illustrated, log profiles are dominated by highly serrate patterns, indicative of thin to medium interbedding of sandstone and mudstone. Core examination confirms this interpretation of log response. Spontaneous potential (SP) profiles typically suggest upward-coarsening textural sequences, but abrupt lower contacts, transitional, upward-fining sequences, and randomly interbedded sequences also are common. Sandstone packets grade seaward into finer and/or texturally immature sequences, which is reflected in the suppressed SP deflection in downdip wells. Although sandy packets thin dramatically basinward, the thinning is directly proportional to the overall thinning of the genetic interval and reflects differential rates of subsidence across and between fault blocks rather than sand-body buildup or pinchout.

Figures 5 through 10 illustrate genetic interval thickness, sandstone distribution, and typical facies sequences as depicted by electrical log profiles for two representative map units. Interval

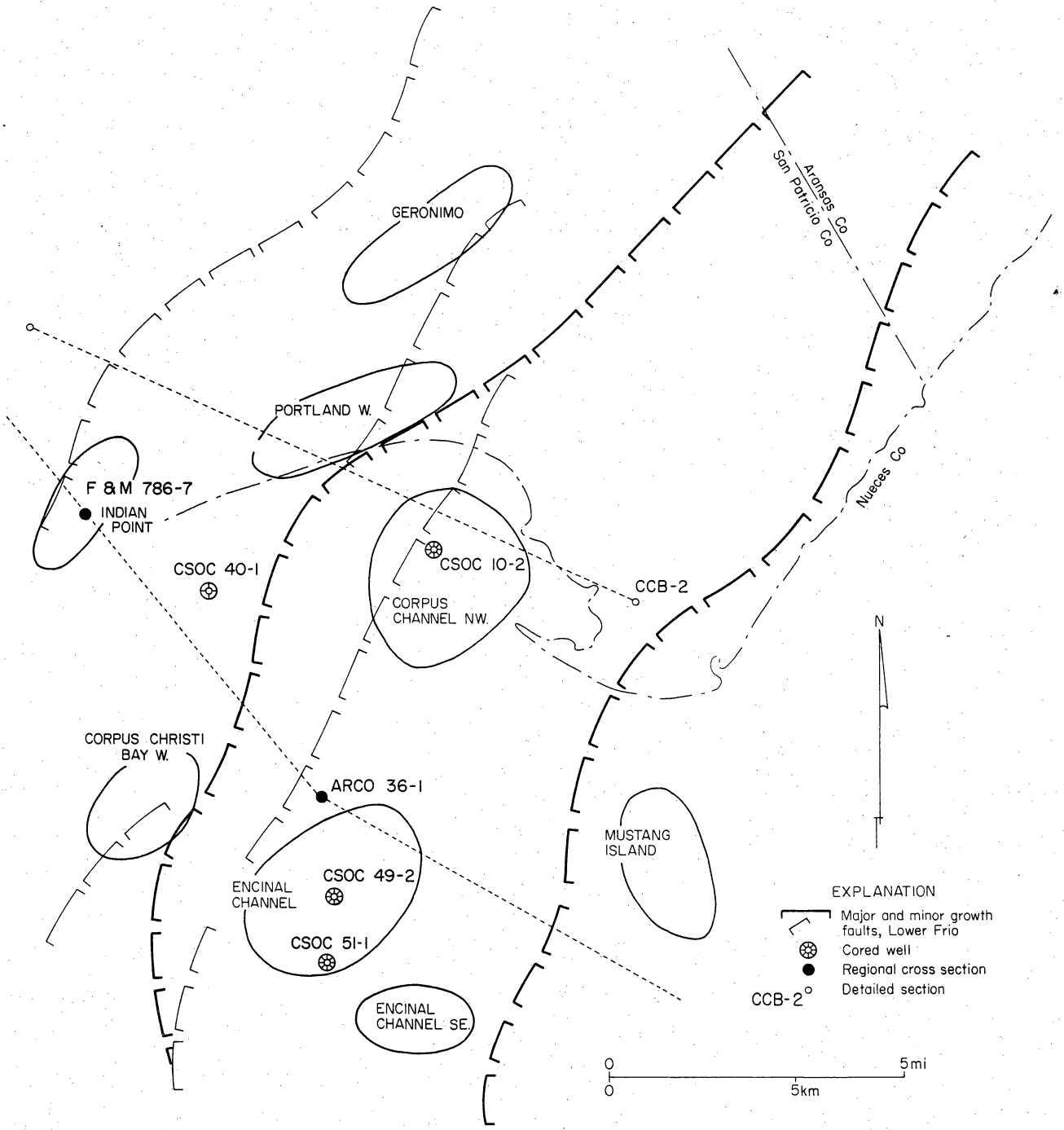

Figure 3. Index map of the Corpus Christi Bay study area showing principal structural features, producing fields, and locations of wells on the regional cross section (Fig. 2) and detailed cross section (Fig. 4).

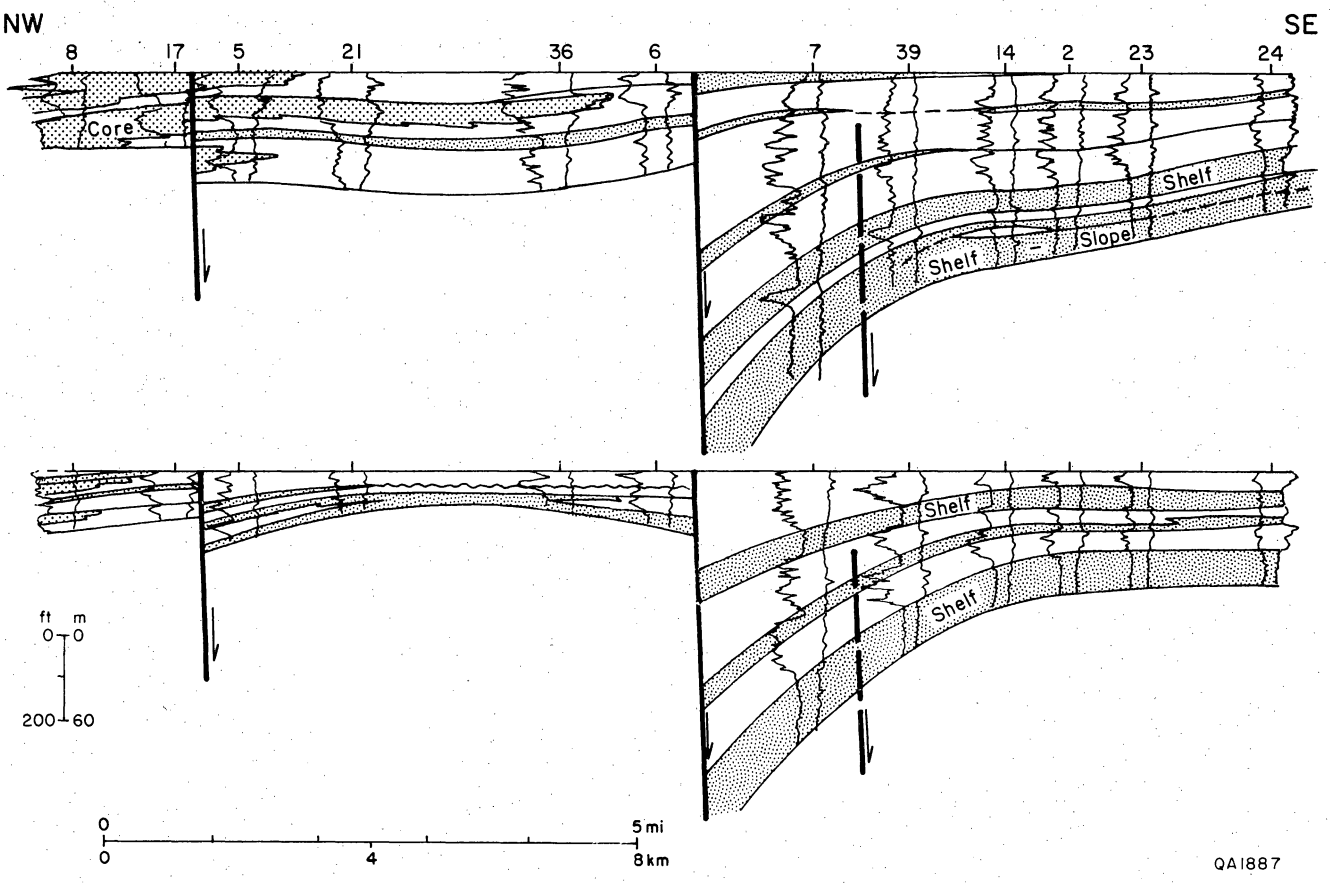

Figure 4. Dip-oriented cross section CCB-2. The section shows two representative facies sequences. The datum for each section is the top of the genetic facies sequence. Note the 5-fold expansion of each sequence across the central growth fault. Marine shelf mudstone units are highlighted to emphasize the sandy packets. From Jackson and Galloway (1984).

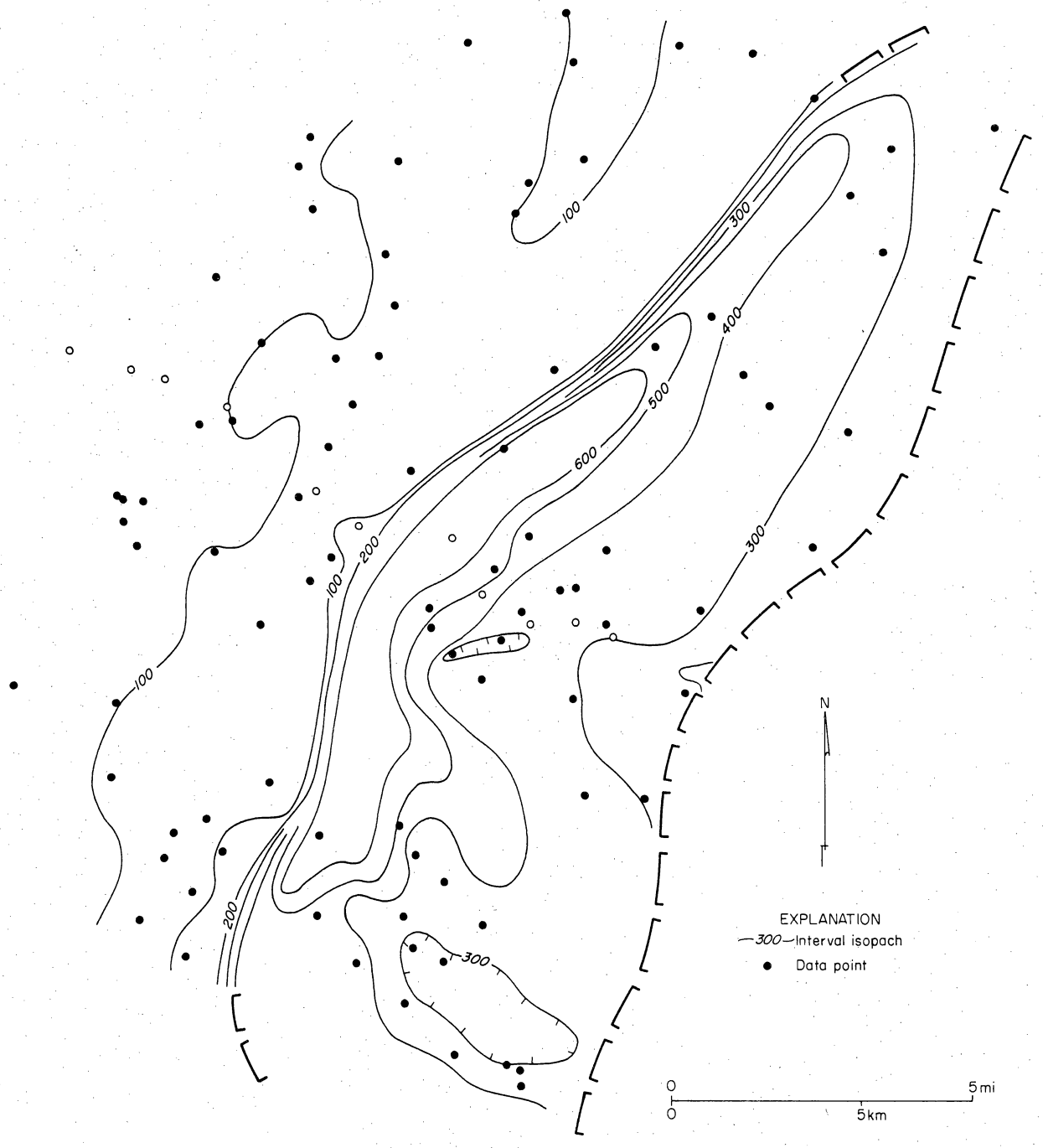

Figure 5. Interval isopach of the lower map unit. Note thickening across the central growth fault.

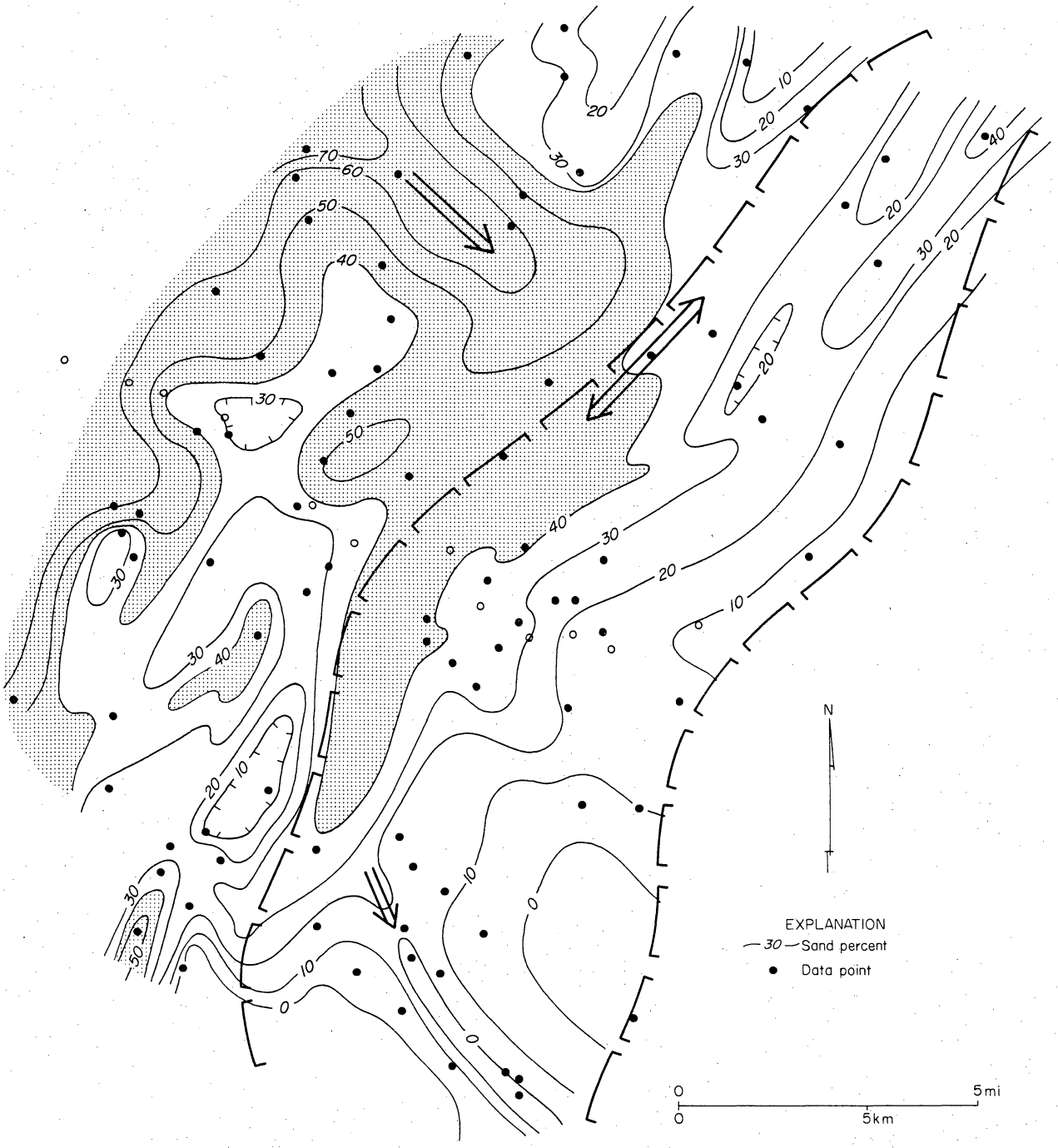

Figure 6. Sandstone-percent map of the lower map unit. Arrows indicate inferred directions of sand transport. Of particular interest is the strike oblique axis indicated by the 20 percent contour at the south margin of the map.

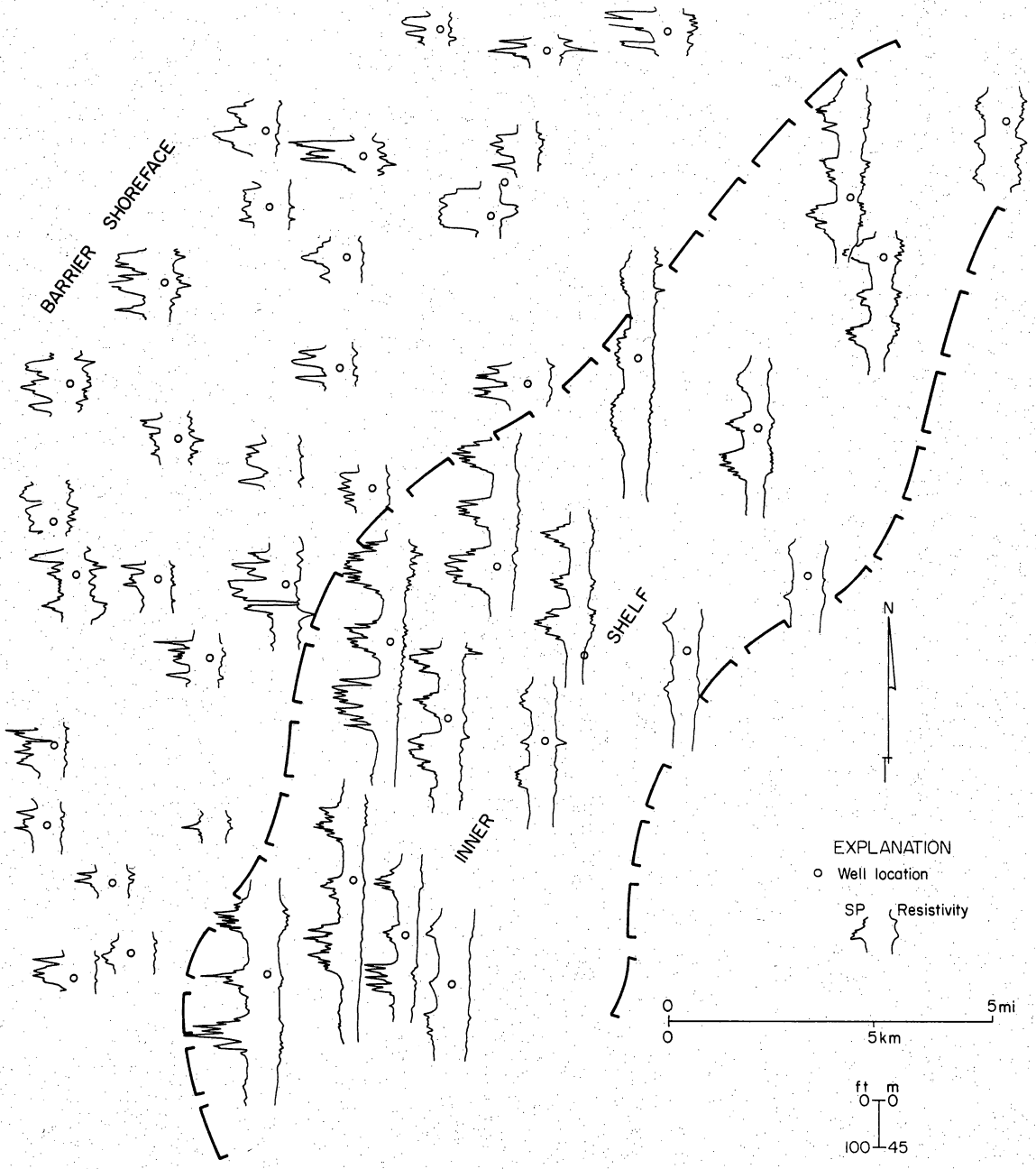

Figure 7. Representative electrical log patterns of the lower map unit. Three well-defined sandstone packages are present in the middle fault block. In the updip block, they are commonly amalgamated to varying degrees and the upward-coarsening pattern is less well defined. Note the massive, blocky pattern typical of the dip-oriented sandstone thick at the northeast quadrant of the map.

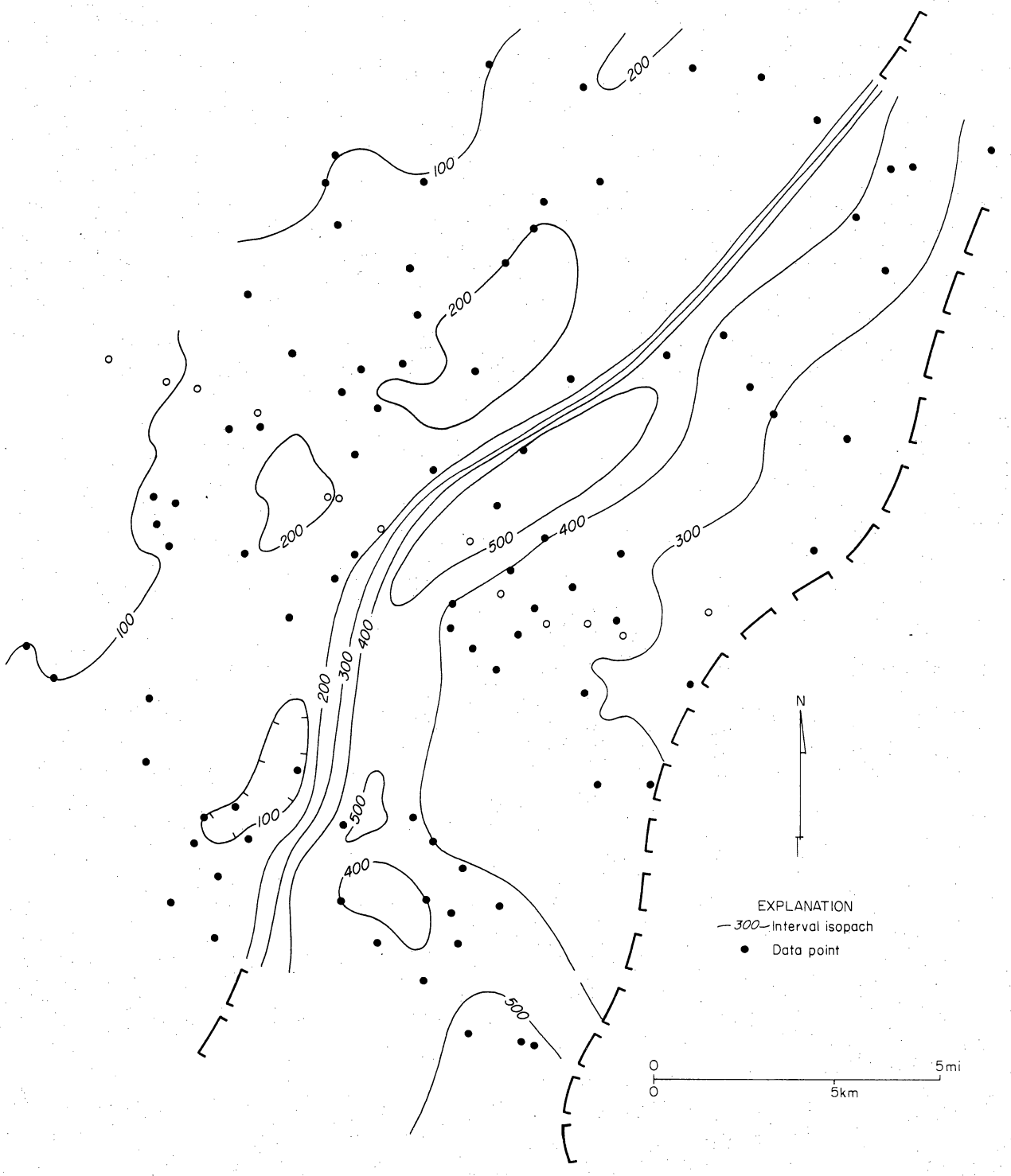

Figure 8. Interval isopach of the upper map unit. Again, note thickening across the central growth fault.

Figure 9. Sandstone-percent map of the upper map unit.

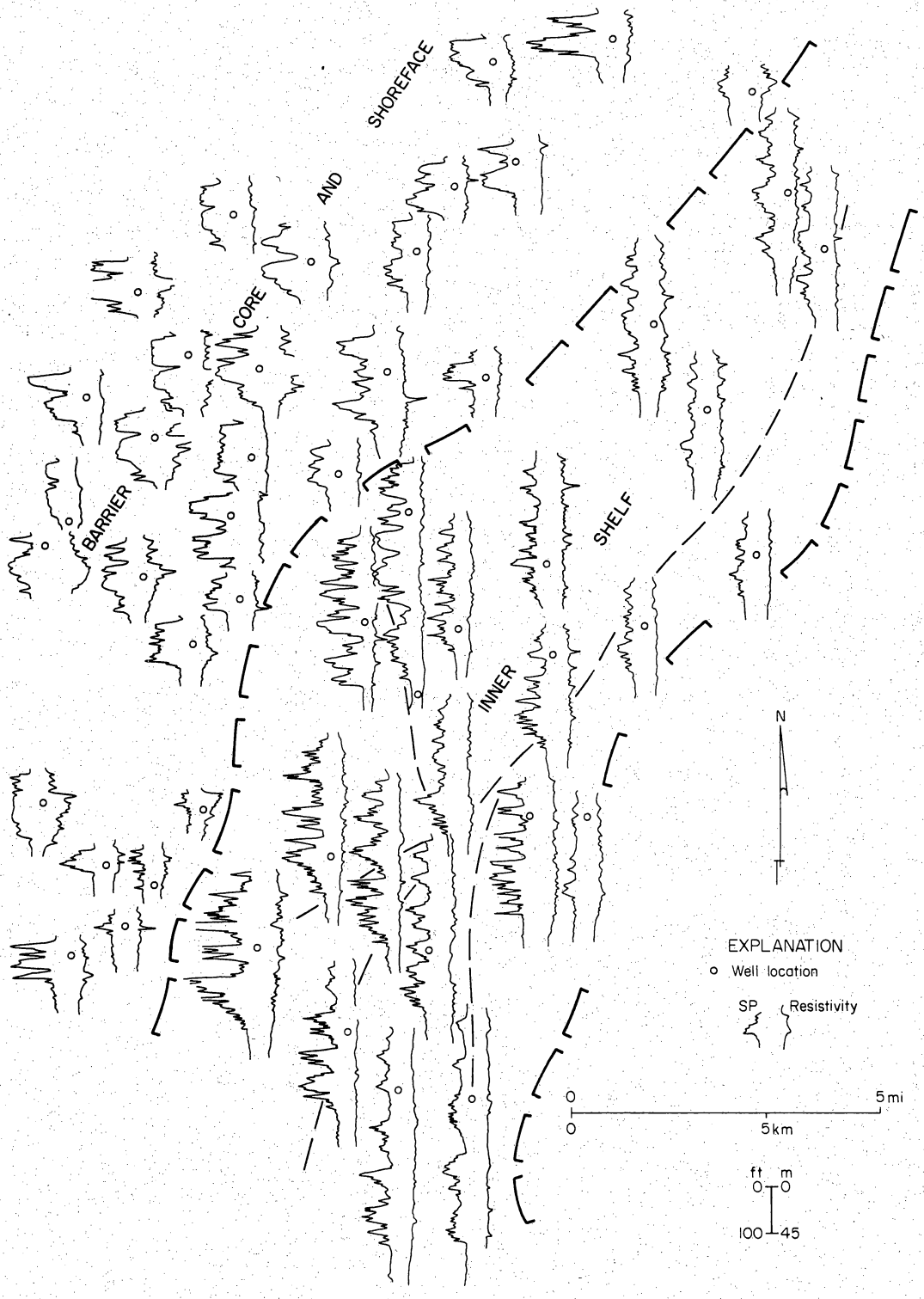

Figure 10. Representative electrical log patterns of the upper map unit. Numerous highly interbedded sandstone packages are present. In the middle fault block, repeated upward-coarsening patterns dominate, indicating transitional inner shelf to distal shoreface deposition. Massive blocky to upward-coarsening patterns in updip wells reflect shoreface to barrier-core sequences winnowed by fair-weather wave reworking.

isopach maps emphasize the abrupt thickness increase across the growth fault that bisects the study area (Figs. 5 and 8). Similar thickness increases likely occur across the downdip fault. To the extent that syndepositional faulting might have influenced bathymetry of the inner shelf, a shore-parallel, elongate trough would result. Perturbations in the generally strike-parallel isopach contours at the south edge of the map suggest a possible oblique spur fault extending between the two master growth faults.

Sandstone percentage maps display similar distribution patterns and exhibit a combination of three distinct facies elements (Fig. 6 and 9):

1. Updip, contours form irregular, strike-parallel trends, and sandstone percentage values are high, commonly exceeding 50 percent. Local sand-rich and relatively sand-poor patches are apparent in the upper map unit (Fig. 6), which shows a broader swath of the sandy barrier island facies because successive progradational shorezones offlap their precursors. The combination of upward-coarsening and blocky log patterns are typical of barrier core, inlet fill, and proximal shoreface sequences in the Frio (Galloway, 1986a). It is noteworthy that, even in the more extensively prograded upper map unit, barrier island sandstone sequences remained updip of the actively subsiding growth-fault bounded basin.

2. Basinward of the barrier island sand belt a series of generally shore-parallel, moderately sandy to sand-poor trends dominate to the downdip limits of mapping. Two generalizations are evident. Overall sand content decreases basinward. On both maps, sand content is generally less than 20 percent at the position of the deep bounding fault. Secondly, sand content is concentrated within the growth-fault defined depocenter that lies in the center of the map area. However, the distribution pattern is complex, and the coincidence of sand-rich areas with isopach thicks is far from perfect, particularly in the upper map unit (Fig. 9). Nonetheless, the coincidence does indicate that the depositional processes responsible for sand redistribution across and along the fore-barrier shelf did tend to focus sand into areas of most rapid subsidence, where it was readily stored. Within this zone, sand sequences form the typical packets, which are separated by correlative shelf mudstone units and are characterized by highly serrate log patterns (Figs. 7 and 10).

3. Between the strike-dominated barrier island and inner shelf depositional elements lie local, dip-oriented sand belts (indicated by the southeast-directed arrows on figures 6 and 9). These digitate protrusions, as defined by the 40 percent sandstone contour, are only a few kilometers long. They merge basinward into strike-parallel, sand-rich belts of the inner shelf trend, and are coincident with areas of particularly high sand percentage values in the updip barrier island trend. Log patterns are transitional between those typical of the barrier and inner shelf facies sequences. Although some log patterns within the belt display sharp bases and blocky log profiles, no prominent scour or channel incision is indicated by detailed cross sections. Rather, the belts apparently reflect an unusual concentration of amalgamated thin to medium sandstone beds with proportionally less interbedded mudstone.

Possible extension of the shore-parallel sandy belts into the next downdip fault block is

speculative. However, an anomalous, narrow, strike-oblique sandy ribbon cuts diagonally across the south end of the middle fault block in the lower map unit, and extends to the limits of well control (Fig. 6). This divergent spur of the more typical strike-parallel shelf sand trend is coincident with the possible cross fault inferred from the isopach map (Fig. 5).

In summary, three principal depositional elements are recognized on the basis of sand body trends and are substantiated by vertical sequences and bedding styles observed on electrical logs. A barrier island sandstone complex (including shoreface, inlet-fill, and barrier core sandstone) lies updip. Downdip, a broad belt consisting of many strike-parallel, sandy axes extends to the basinward limit of well control. Between the two are local, digitate, dip-oriented sand axes that merge both updip and downdip into the shore-parallel sandstone facies.

Three distinct, commonly interbedded facies assemblages can be recognized in conventional cores of distal barrier and shelf deposits of the Corpus Christi Bay area:

1. Storm-bedded, distal shoreface/inner shelf sandstone forms the bulk of the mapped sandstone units that lie basinward from massive, barrier-core sand bodies. The dominant feature of this facies is the presence of numerous, stacked and amalgamated storm beds. A logical, persistent genetic boundary between the shoreface and adjacent shelf deposits cannot be defined in the core sequences; both environments are considered to be gradationally related sites of deposition of this facies assemblage.

2. Inner shelf sandstone and siltstone is commonly gradationally interbedded with the shoreface/shelf sandstones.

3. Shelf siltstone and mudstone constitutes the bulk of the muddy sequence containing the Frio shelf sandstone units.

These facies assemblages and, for comparison, the barrier core facies are described below.

Barrier Core Sandstone.--The Frio barrier-core facies assemblage includes shoreface, inlet-fill, and beach sandstones (Galloway 1986a). The sandstones have fine to medium grain sizes that are well sorted. Massive to thick-bedded units exhibit tangential cross stratification, planar lamination, and structureless intervals. Burrows are common and include *Ophiomorpha* and *Scoyenia*. Root traces occur locally near the top of the sequence. Minor components include fragmented plant debris and a variety of shell material, including oysters.

Storm-Bedded Distal Shoreface/Shelf Sandstone.-- Thin to medium beds of very fine to fine well-sorted sandstone containing thin interbeds and drapes of burrow-churned siltstone and mudstone characterize the distal shoreface to inner shelf transitional facies assemblage (Figs. 11 and 12). Sandstone beds typically display sharp upper and lower contacts. There is little evidence of basal erosion, but siltstone and mudstone clasts are common. Upward-fining beds are a recurrent, but not dominant textural trend. Burrow density commonly increases in the top of thicker beds. Scale of bedding units ranges from a few cm to approximately one meter (3 ft); thickest units may reflect amalgamation of multiple depositional events. Bed thickness decreases basinward from the shoreface to the inner shelf. Sedimentary structures include abundant low-angle to planar lamination (Figs. 11, 12, and 13), low-angle ripple to wavy cross-lamination, and minor ripple and deformed lamination. Some rounded, low-angle cross laminae suggest that hummocky cross-stratification may be locally present. Biogenic structures are abundant and diverse (Figs 11, 12, and 13). Common forms include a variety of ill-defined *Scoyenia*-like tubes, *Teichichnus, Ophiomorpha, Thalassinoides,* and *Planolites*. Together this cruziana assemblage is typical of neritic environments (Seilacher, 1978). Minor constituents include fragmented plant debris and thin-shelled pelecypod and gastropod fossils.

Sandy, storm-bedded units commonly form the upward-coarsening packages that lie a few

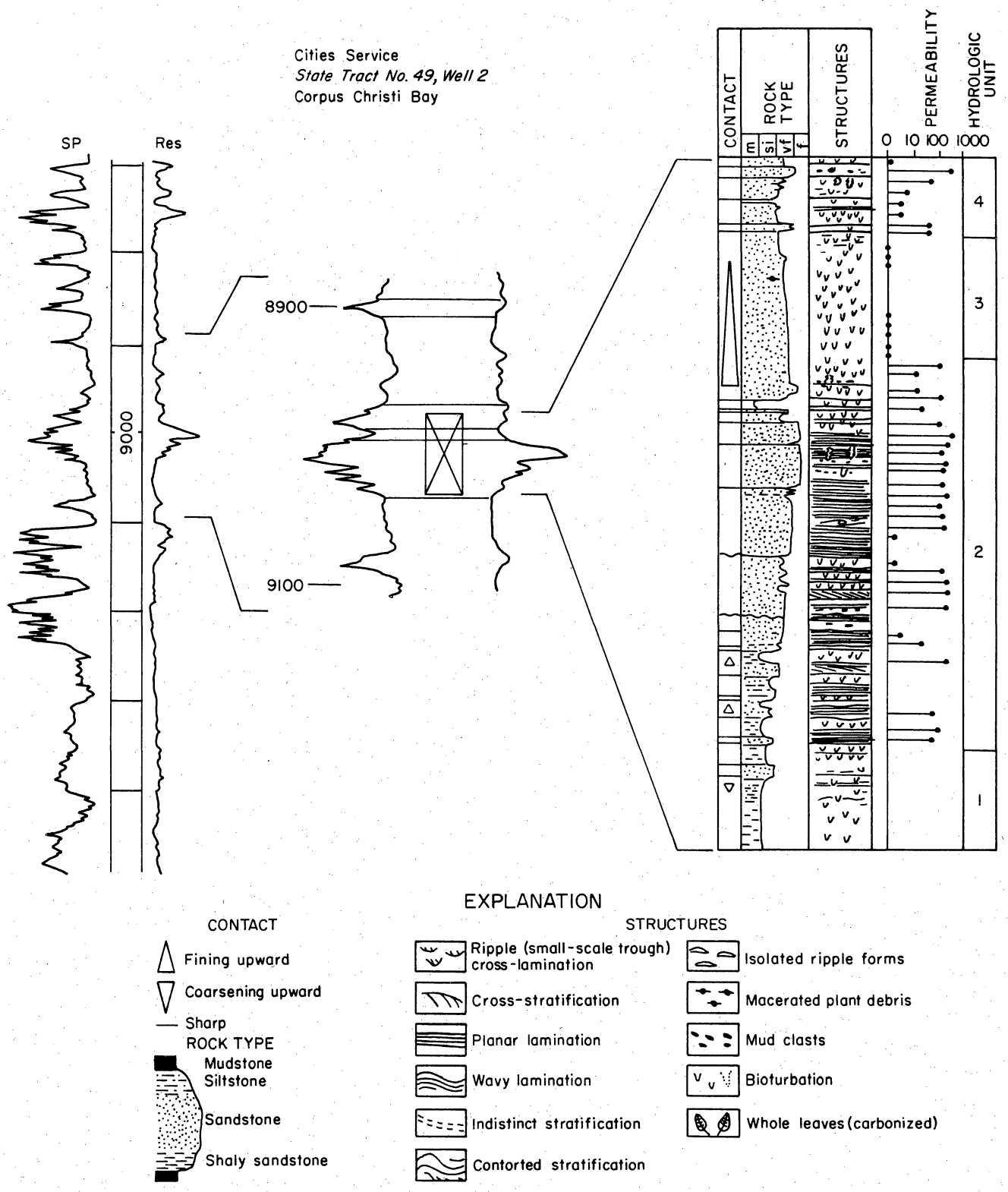

Figure 11. Stratigraphic setting, log pattern, textural sequence, and internal features of an upward-coarsening/upward-fining distal shoreface sandstone sequence. Storm-bedded very-fine to fine sandstone is bounded above and below by inner shelf burrowed sandstone. Core is from the K-8 reservoir interval.

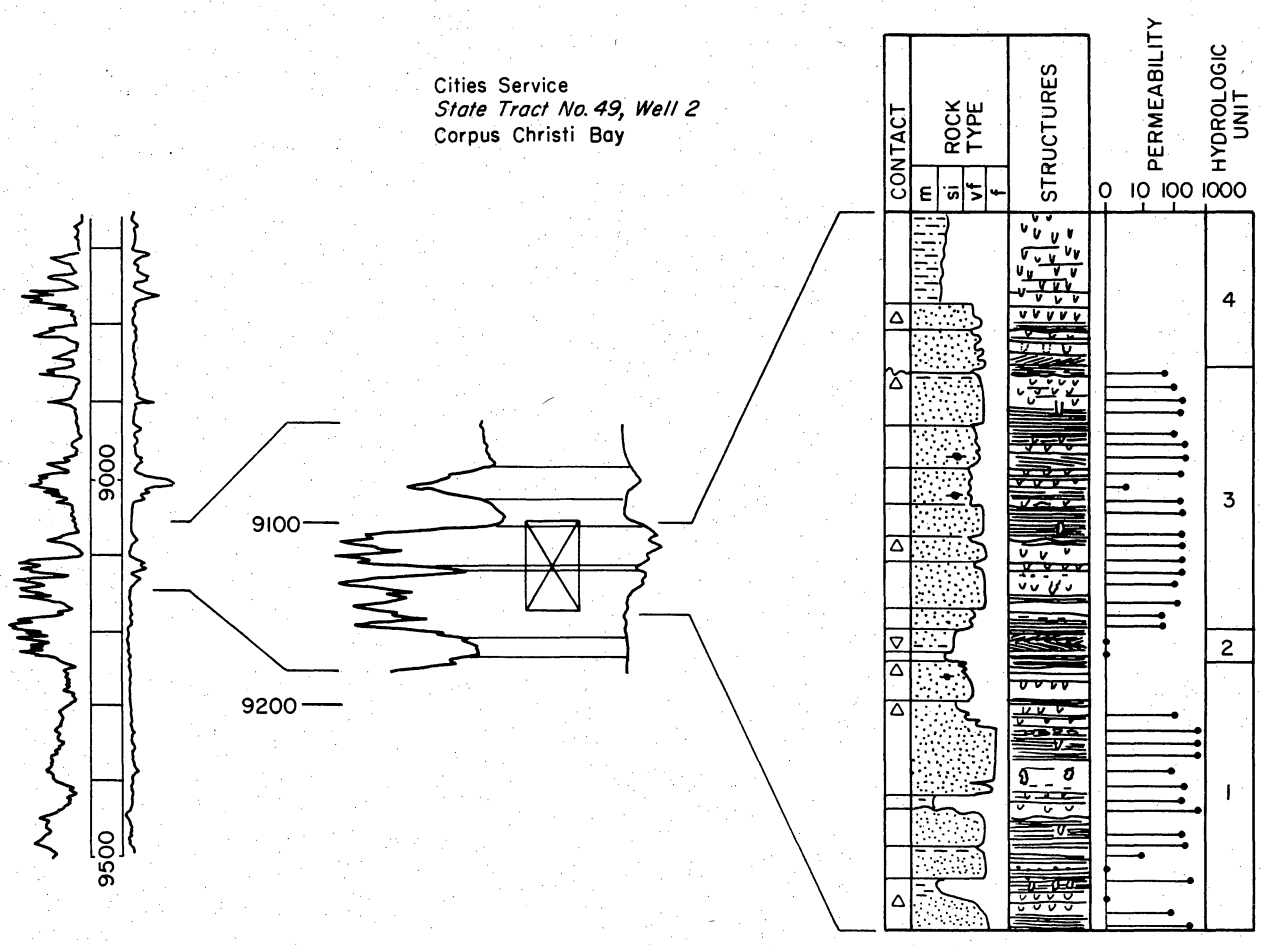

Figure 12. Stratigraphic setting, log pattern, textural sequence, and internal features of a stacked series of distal shoreface/inner shelf storm beds. Note the heterogeneous but common primary laminations. For explanation of core symbols, see figure 11. Core is from the L-1 and L-2 reservoirs.

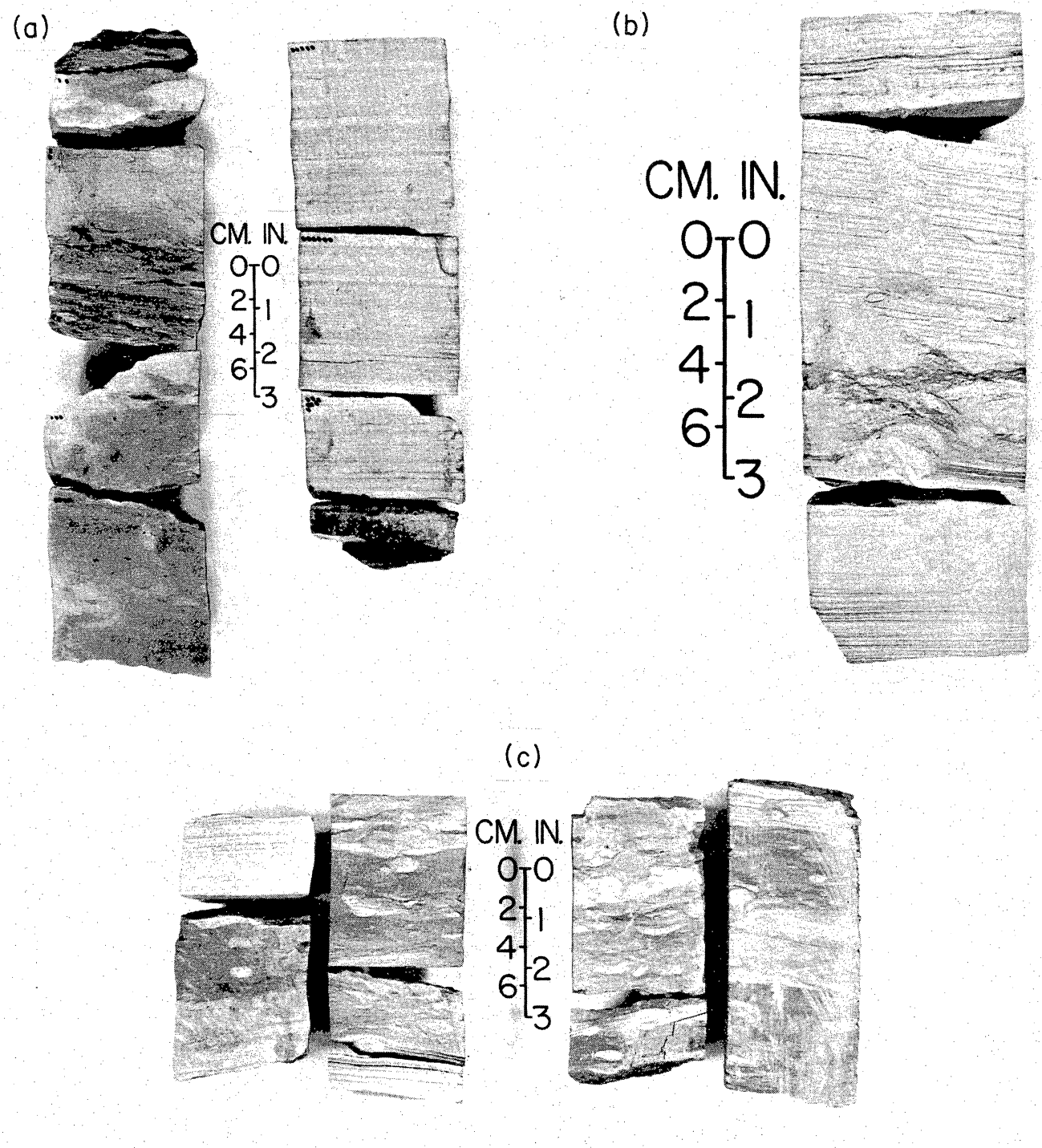

Figure 13. Typical features of Frio storm-bedded sandstones and associated inner shelf arenites. A. Parallel to low-angle cross-laminated fine sandstone interbedded with burrow-churned to faintly laminated muddy siltstone. Note sharp upper and lower contacts of the sand bed. B. Distinctly planar- to low-angle cross-laminated storm sandstone beds. Lamination is disrupted by prominent walled and unwalled burrows. Lower bed contains fewer silty laminae at the top. No textural trend is present in the thicker upper bed. C. Burrowed, muddy siltstone and thinly interbedded, parallel laminated very-fine sandstone units typical of the inner-shelf facies sequence.

kilometers seaward of massive barrier-core sandstone bodies (Fig. 4), and are best developed on the down-thrown sides of contemporaneous growth faults. Despite their interebedded character, which readily suggests strongly punctuated deposition, sandstones of this facies form dominantly shore-parallel ribbons and belts.

Inner Shelf Burrowed Siltstone to Sandstone.-- Thin- to thick- bedded, burrow-churned sandy to muddy siltstones and very fine sandstones were deposited seaward and marginal to the storm-bed facies (Fig. 14). Intense bioturbation characterizes the facies; a diverse assemblage of trace fossils includes *Skolithos, Teichichnus, Thalassinoides, Planolites, Ophiomorpha, Rhizocorallium,* and *Diplocriterion.* This association indicates neritic water depths (Seilacher, 1978). Contained within the burrowed siltstone and very fine sandstone are distinct, sharp-based beds of very fine, laminated sandstone typical of the distal-shoreface/inner-shelf storm beds (Figs. 13 and 14). These beds record unusually widespread redistribution and reworking of sand from the shoreface by major storm events. Locally, sandstones are fossiliferous and contain calcite cement; finely fragmented plant material also occurs in some beds.

Shelf Siltstone.-- The sand-rich framework facies of the Frio barrier-to-shelf facies tract are contained within a matrix of sandy to muddy siltstone that is thoroughly burrowed (Figs. 15 and 16). Texturally monotonous sequences of burrowed siltstone to very-fine sandstone are interrupted by thin beds of parallel to wavy-laminated very fine sandstone, which are distal or minor storm beds. Burrows are dominated by nondescript *Scoyenia*-like forms along with *Helminthoida* and *Thalassinoides*. Faint wavy and ripple laminations are preserved in some burrowed zones. Pelecypod fossils also occur.

Frio Shelf Depositional Processes

The sandy, distal shelf and inner shelf sandstone reservoirs of the Frio Formation in the Corpus Christi Bay area were produced by the periodic redistribution of shoreface sand onto the inner shelf. This lateral transport occurred as a result of storm-induced bottom-return flow (locally channelized or focused by inlets or shoreface topography) and the more continuous alongshore reworking by wind-forced geostrophic flow (Fig. 17). The processes and sedimentary products are directly comparable to those of the storm-dominated Holocene Texas shorezone and inner shelf (Fig. 18, Morton 1981) and to the middle Atlantic shelf (Swift et al. 1986a, Wright et al. 1986). Sand packages (though not necessarily individual sand beds) remained attached to the shoreface, and constitute a contiguous distal shoreface and inner shelf facies assemblage. However, storm-induced geostrophic currents redistributed much of the sand, which was suspended by wave-orbital currents, into strike-elongate belts of cleaner, thicker fine to very fine sand beds. Parallelism between depositional patterns and growth fault traces (Figs. 6 and 9) suggests that minor perturbations in shelf morphology that focused or influenced the bottom current flow field were created by differential movement along

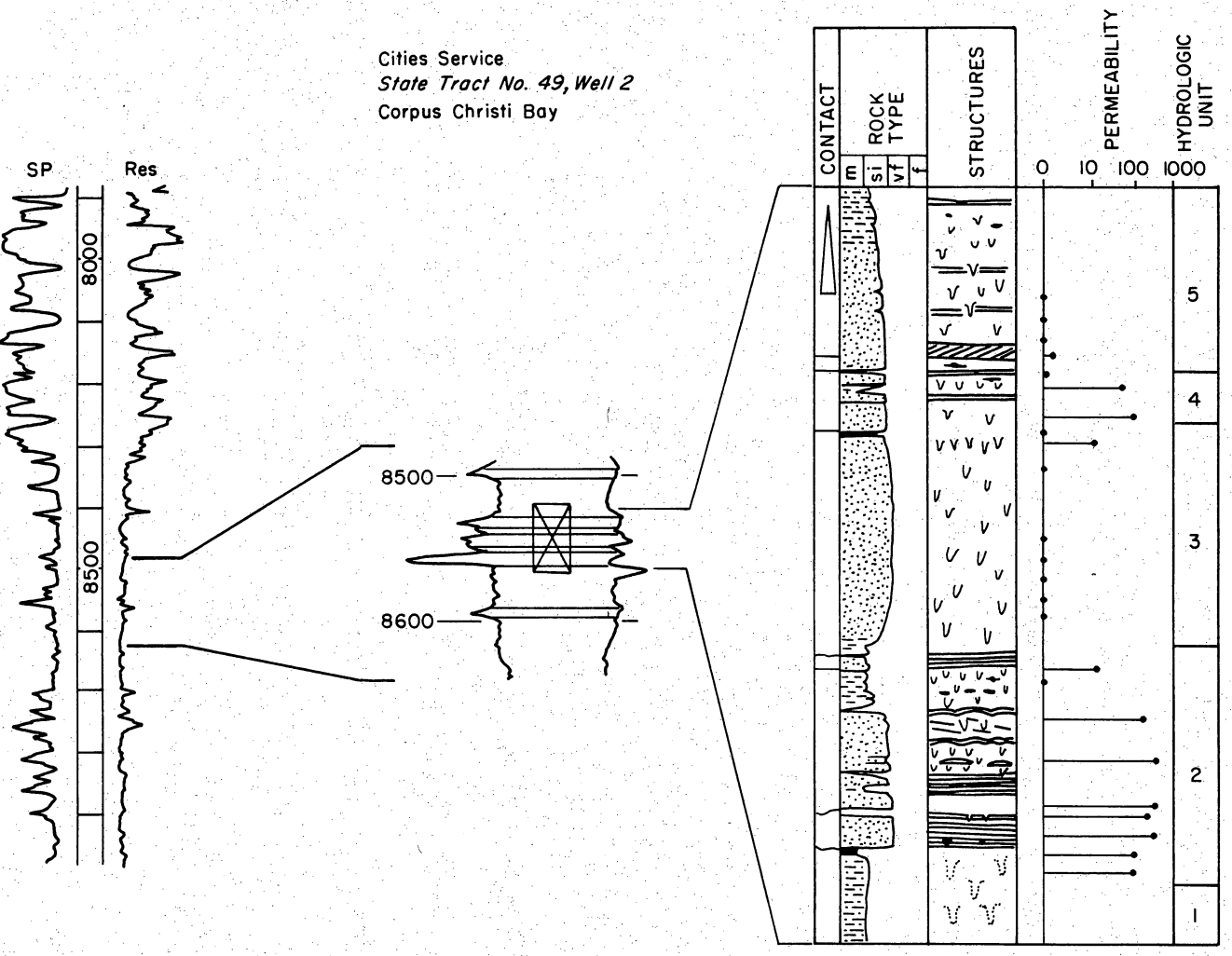

Figure 14. Stratigraphic setting, log pattern, textural sequence, and internal features of the inner shelf sandstone and siltstone facies assemblage. Thin, laminated storm beds are prominent in the lower third of the core. For explanation of core symbols, see figure 11. Core is from the J-3 reservoir interval.

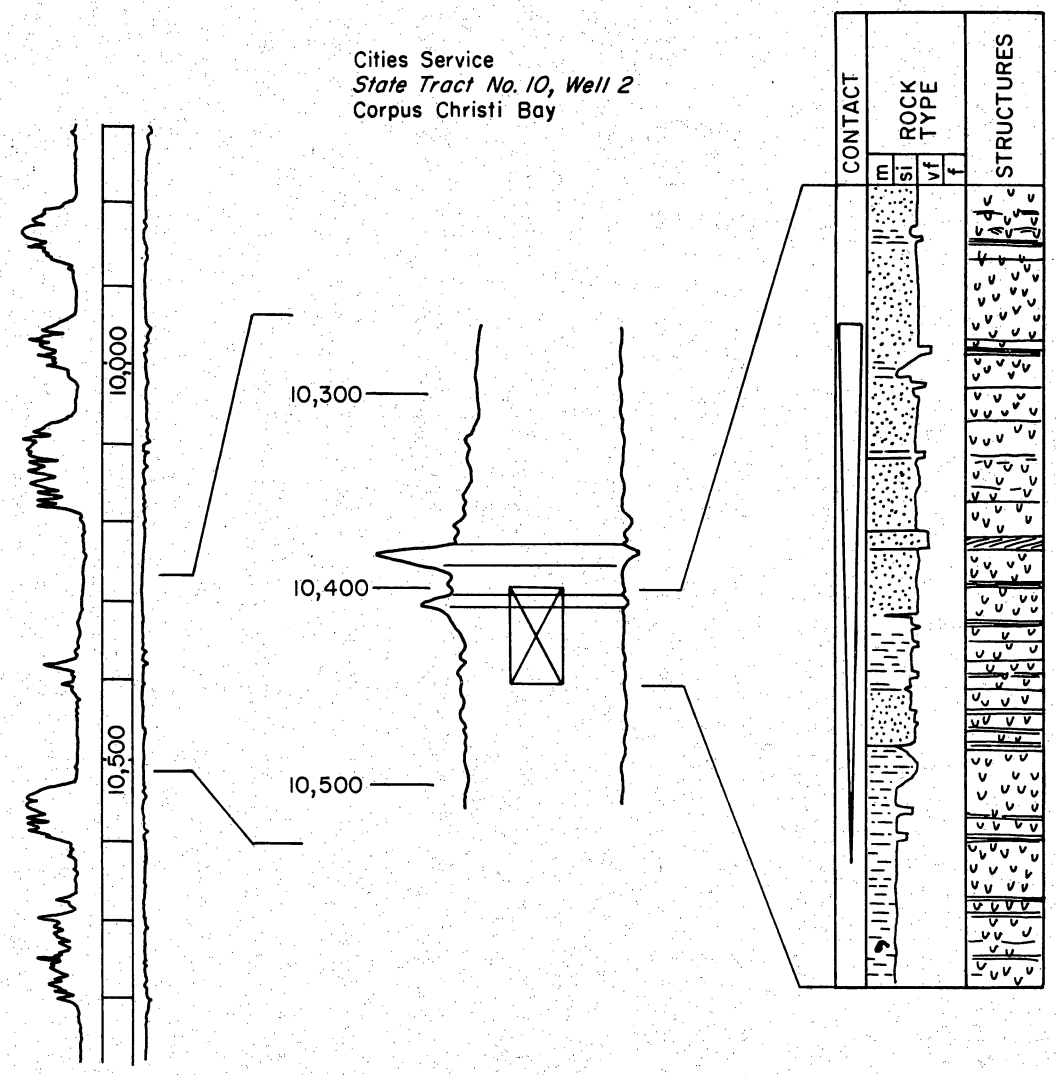

Figure 15. Stratigraphic setting, log pattern, textural sequence, and internal features of the shelf siltstone facies. Burrows dominate the sedimentary structures, but thin interbeds of laminated very-fine sandstone are preserved distal storm layers. For explanation of core symbols see figure 11. Core is between the M-2 and M-3A reservoirs.

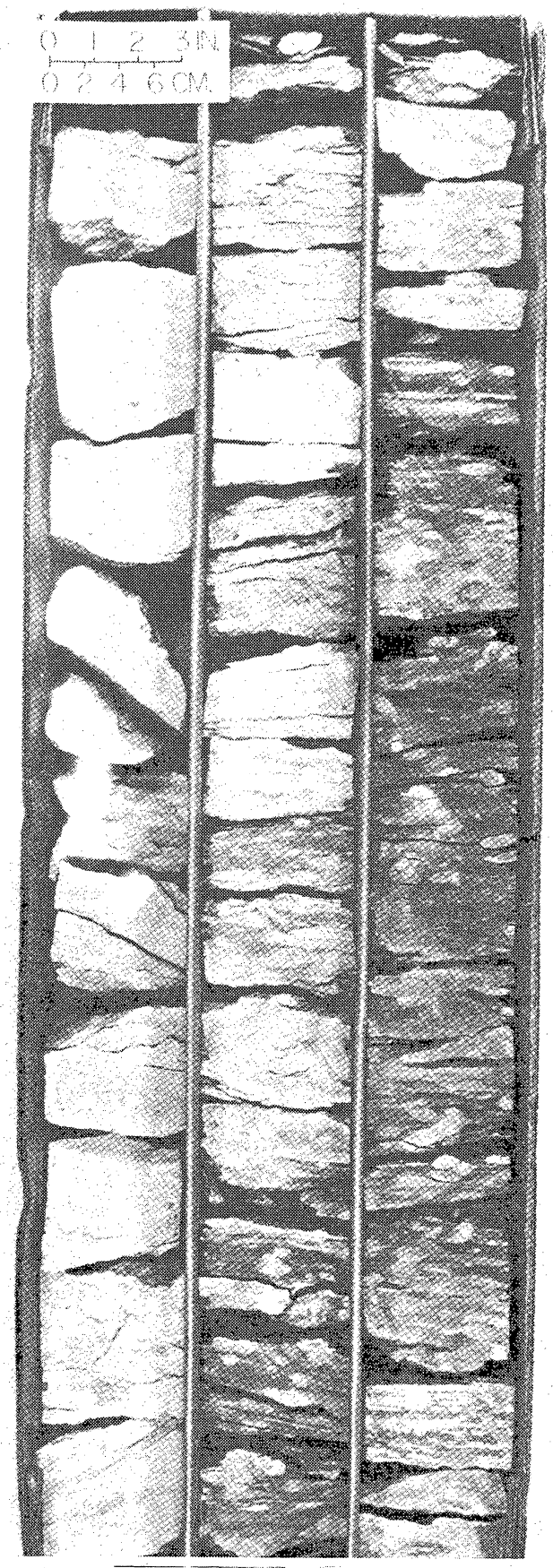

Figure 16. Core photograph showing typical features of muddy siltstone to sandy siltstone (top of core) of the shelf facies.

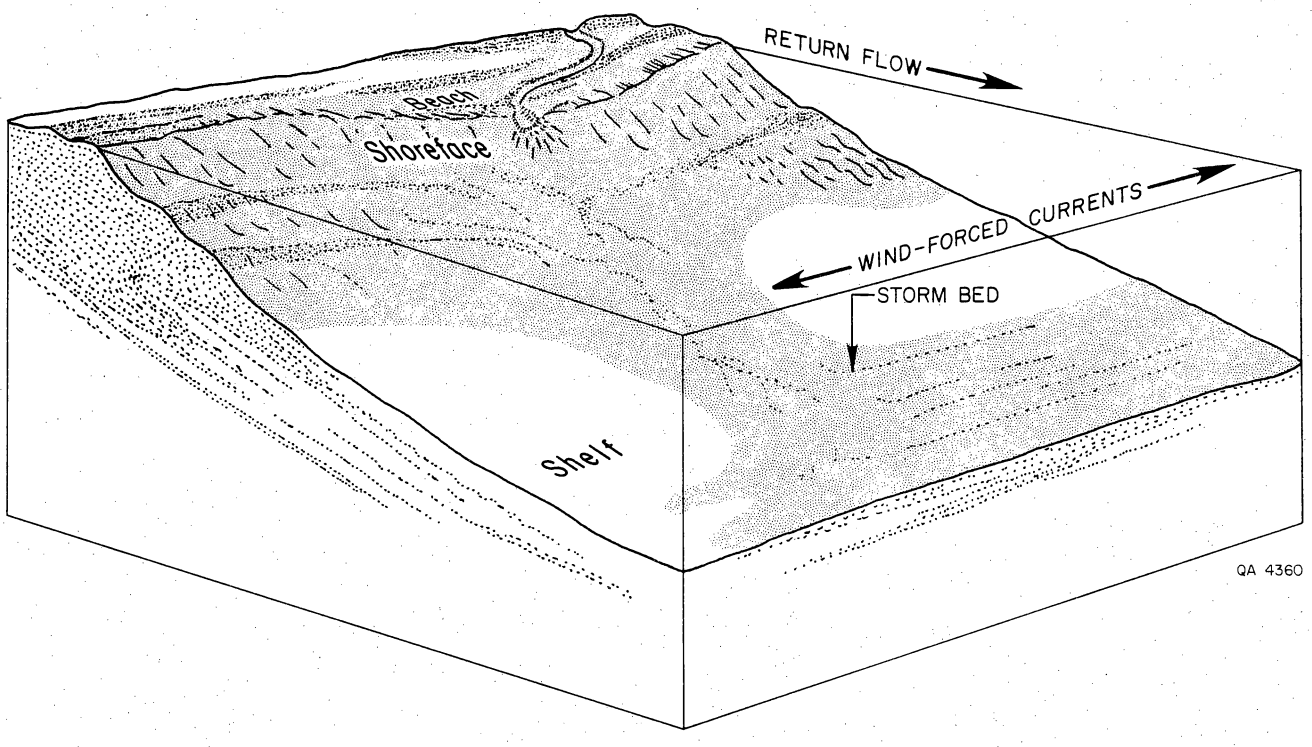

Figure 17. Depositional setting of the Frio distal-shoreface to inner-shelf sandstone sequences. Storm-induced bottom-return flow swept sands from the fairweather shoreface across the lower shoreface and onto the inner shelf. During the same or subsequent storms, wind-forced bottom currents reworked the sands into amalgamated, shore-parallel sheets or belts. The drawing shows the nearshore setting of storm bed deposits such as those illustrated in figures 11 and 12.

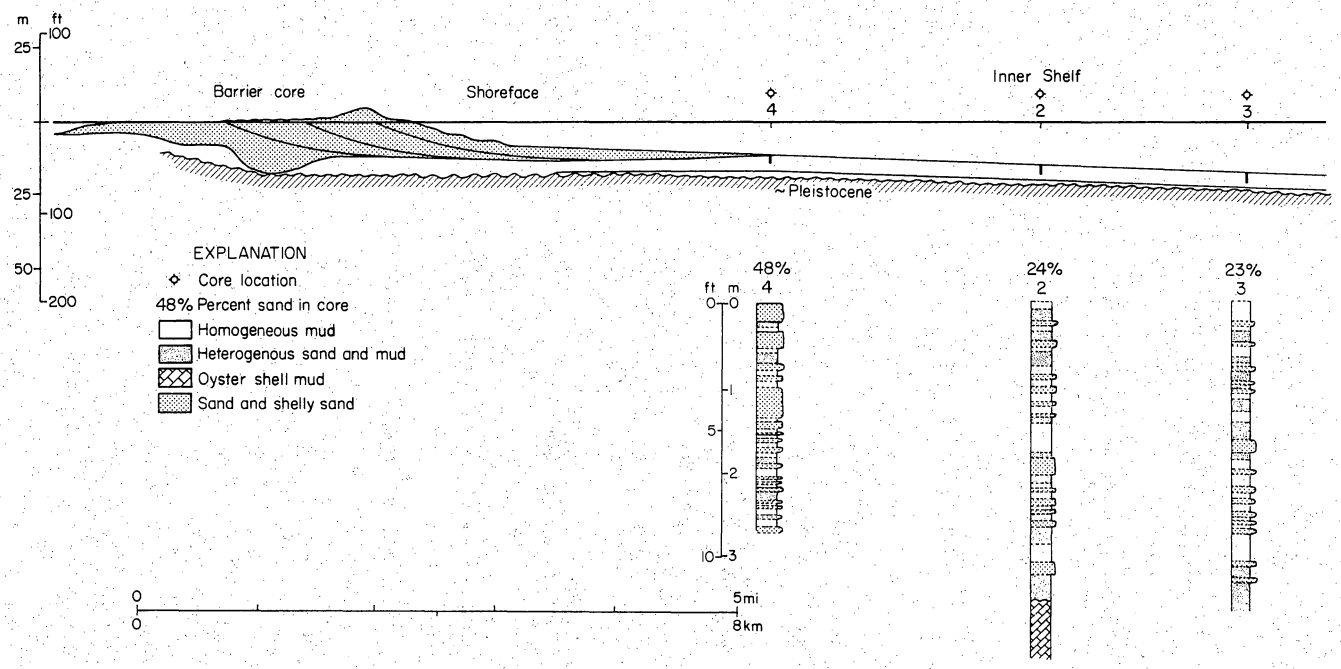

Figure 18. Depositional setting of Holocene shelf storm beds with respect to the adjacent barrier island sand body. Barrier island geometry is from Wilkinson (1975) and McGowen and Morton (1979) and storm bed sequences are from Morton (1981).

faults. During fairweather periods, sediments below wave base were wholly to partly reworked by marine burrowing organisms. Upward-coarsening sequences were produced as the shoreface prograded basinward, and increasingly proximal storm deposits were superimposed on distal deposits. Evidence of large-scale accretion or bar migration is lacking, and sand bodies display sheet geometries rather than bar-like geometries. We infer that the inner shelf sands formed low relief shoals rather than discrete sand ridges, which are common along higher-energy coasts having coarser grain sizes (Swift et al. 1986b).

The prominent shore-parallel sandstone distribution pattern, combined with the heterogeneous nature of textural and structural sequences within individual beds, confirms that storm-related wind-forced currents were the most likely agent of sand redistribution onto and across the inner Frio shelf. Although similar Frio sandstone sequences were interpreted by Berg and Powell (1976) to be the product of turbidity currents, this interpretation is rejected for several compelling reasons: (1) The original model for a storm-generated shelf turbidite (Hayes 1967) has been discredited by subsequent analysis of modern storm-related shelf processes of the Texas coast (Morton 1981). (2) The predominance of traction transport of sand is abundantly indicated by the pervasive lamination and cross-lamination within sands and the observed sediment textures and structures are typical of shelf storm beds (Aigner 1985, Swift et al. 1986b). (3) Vertical sequences of lamination types are best characterized as near-random (examine for example figures 11 and 12), reflecting the variable current directions inherent in storm passage. (4) Although interbedding of fine and coarse units is indicative of punctuated deposition, interbedding itself conveys no significance as to depositional process. As pointed out by Zeller (1964), interbedded coarse/fine sequences are inherently cyclic, but such cyclicity is of no genetic or mathematical significance. (5) Several authors (Parker 1982; McCave 1985) point out that sandy shelf turbidites are "dynamically unreasonable and unnecessary to explain modern shelf data". (6) Finally, gravity-driven turbidity flows cannot explain the propensity for longshore transport and resultant strike-dominant sandstone distribution patterns.

Petrography

Thin sections of five lower Frio reservoirs (J-2 through K-2 reservoir interval) in the West Mustang Island field (Fig. 3) show that the distal shoreface and shelf sandstones are moderately-sorted to well-sorted, fine to very-fine grained arkoses containing substantial amounts of volcanic rock fragments. Within the producing field, the composition of several sandstone bodies over a depth interval of 300 m (3155-3469 m) is relatively uniform as shown by the range and average of the three principal components: quartz (37 to 62%, average 42%), feldspar (20 to 40%, average 33%), and rock fragments (7 to 16%, average 10%). Minor accessory minerals in these marine sandstones are mica and glauconite pellets, which were identified in all but one sample. In addition to the framework grains, cements normally account for about 1 to 6 percent of the total rock volume. Authigenic cements include quartz and plagioclase overgrowths, pore filling kaolinite, and sparry calcite. The textures, mineralogy, and overall composition of these reservoir sandstones are comparable to those reported by Loucks et al. (1986) for Frio and other Tertiary sandstones of the middle Texas coast.

Visual porosities of these geopressured sandstones range from 6 to 33 percent but most of the measured values are between 20 and 28 percent. Such unusually high porosities at intermediate depths are a result of well developed secondary porosity that ranges from 6 to 17 percent and accounts for slightly more than half of the total porosity. This pervasive secondary porosity, which prevents the rocks from being extremely tight, formed mostly by dissolution of feldspar and possibly leaching of some calcite cement. Because of this diagenetic relationship, creation and enlargement of voids by preferential leaching are chiefly related to bulk mineralogy, especially the abundance of feldspar, and do not depend on the abundance or distribution of original porosity. Secondary porosity is recognized on the basis of intragranular voids, oversized pores, packing inhomogeneities, and relict clay rims. The fact that these thin clay coatings remain after the feldspar grains are dissolved may partly explain why the permeabilities of many core samples are low even though the combined primary and secondary porosity is high.

Authigenic cements and deformed rock fragments are two components that commonly occlude porosity and modify interstitial connections within the Frio sandstones. Quartz and feldspar overgrowths generally reduce the sizes of pores and thereby restrict flow whereas authigenic kaolinite and mashed rock fragments normally fill the entire pore and create barriers to fluid movement. Additional microscopic heterogeneties occur as laminae of deformed mudstone clasts surrounded by sand grains that are moderately well sorted. The abrupt changes from non-porous fine-grained laminae to highly porous coarser-grained laminae cause flow discontinuities that are expressed as variations in the vertical distribution of porosity and permeability.

Spatial Variations in Pore Properties

Total porosities of Frio sandstones agree within a few percent regardless of whether they are

determined from point counts of thin sections or derived from conventional core analyses. This close agreement demonstrates that standard laboratory measurements are accurate enough to determine spatial variability of pore properties from the hundreds of porosity and permeability values available for reservoirs in the Corpus Christi Bay area. The large number of measurements from numerous wells permits spatial comparisons at two different levels; vertical profiles for individual sandstone sequences and subregional lateral variations within correlative sandstone units.

Intrawell Heterogeneities.-- Plots of porosity and permability for three cored intervals in the Cities Service State Tract 49 No. 2 well (Figs. 11, 12, and 14) illustrate the macroscopic heterogeneity within the reservoirs and provide the basis for interpreting the hydrologic units that control the efficiency of drainage and ultimate hydrocarbon recovery. These intrawell heterogeneties largely determine the productive capability of a well regardless of the overall reservoir quality.

The K-8 reservoir (Fig. 11) is a thick amalgamated sequence of thin-bedded siltstones and fine sandstones that display an upward-coarsening and upward-fining facies architecture. These distal shoreface and shelf deposits are vertically arranged so that they form four distinct hydrologic flow units. From bottom to top, units 1 and 3 are moderately porous but impermeable zones that are wavy laminated to structureless and homogenized by burrowing. The thickest hydrologic unit, which occupies the central portion of the sand body, is highly porous and moderately to highly permeable fine- to very fine-grained sandstone. The sandstone is cross bedded to horizontally laminated with slight burrowing, but the burrows are restricted to thin, isolated intervals. A unit having high porosity and variable permeability (unit 4) caps the sequence. This uppermost unit is composed of very fine-grained sandstone that is both laminated and burrowed (Fig. 11). The vertical arrangement of highly permeable flow units makes the K-8 sandstone an excellent reservoir with about 66 percent of its thickness having permeabilities adequate to sustain high rates of fluid production.

Although the superimposed L-1 and L-2 sand bodies are both composed of upward- coarsening beds (Fig. 12), their vertical complexity confirms that they are separate reservoirs; a fact established by differences in bottom-hole pressures and production characteristics. The L-2 reservoir is an amalgamation of thin-bedded fine- to very fine-grained sandstones that were deposited in distal shoreface environments. Together the beds form three hydrologic units. Both the lower and upper flow units are highly porous. The lower unit has variable permeabilities due to the alternating burrowed to horizontally laminated zones containing mudstone clasts. In contrast, the upper unit is highly permeable because horizontal, ripple, and wavy laminations are preserved. The thick upper hydrologic unit is slightly bioturbated, but the zones of burrowing are restricted in thickness. A thin zone of low porosity impermeable shelf mudstone separates the upper and lower flow units of the L-2 reservoir. Overall, the L-2 sandstone has excellent reservoir characteristics including moderate permeabilities near the top and adequate permeabilities for about 84 percent of its thickness.

The L-1 reservoir is composed of stacked upward-coarsening and upward-fining siltstones and very fine-grained sandstones deposited in distal shoreface and shelf environments. The reservoir is

subdivided into three hydrologic subdivisions, each with different reservoir quality. The thick, moderately porous, but impermeable lower and upper units are wavy laminated to structureless and thoroughly bioturbated shelf mudstones similar in composition and character to the flow barrier in the L-2 reservoir. The middle hydrologic unit is highly porous but has low permeability due to burrowing of the ripple to parallel laminated beds. Considered together, the three hydrologic units make a poor reservoir because the upper unit is impermeable and less than 10 percent of the total thickness has moderate to high permeabilities.

One of the most heterogeneous reservoirs, the J-3, occurs at the base of an upward-coarsening sequence (Fig. 14) and is composed of alternating moderately sorted very-fine grained sandstone and siltstone beds. The stratigraphic position and sedimentary structures of the J-3 reservoir indicate that it formed on the inner shelf as an amalgamated storm-bed deposit. This reservoir is composed of five different hydrologic units, but only two of the units, or about 30 percent of the total thickness, are sufficiently permeable to deliver fluids at acceptable rates of production. Hence this reservoir is not very productive. The bottom unit (unit 1), which has low porosity and no measurable permeability, is a structureless to faintly wavy laminated siltstone that is thoroughly burrowed and contains a layer of transported broken shells. Units 2 and 4 are highly porous and moderately to highly permeable very fine-grained sandstones with faint low-angle cross bedded laminations. The intervening unit 3 and overlying unit 5 are moderately porous but impermeable siltstones which are flow barriers because they are structureless and intensely bioturbated.

Interwell Heterogeneities.-- Maps of average permeabilities for the J-3, K-8, and L-2 reservoirs (Figs. 19, 20, and 21) illustrate the magnitude of megascopic heterogeneities over a large area. Such large-scale interwell variability is mostly related to sandstone properties inherited from the original depositional environment rather than to subsequent diagenetic modifications.

Despite being composed of thin beds alternately dominated by physical structures and burrows, the J-3 reservoir typically has moderately high average permeabilities (Fig. 19) between 150 and 200 md. High average permeabilities occur throughout this thin sand body regardless of its position with respect to the major bounding faults (Fig. 19). Most wells penetrating the J-3 reservoir have maximum permeabilities of at least 400 md and two wells in the Corpus Channel field each have maximum permeabilities of more than 1 darcy. Intermediate and low average permeabilities are limited to narrow elongate zones with northeast-southwest orientations. The J-3 reservoir in the State Tract 49-2 well (Fig. 14) has maximum (605 md) and average (222 md) permeabilities that are typical of this sandstone.

In contrast, the K-8 reservoir generally has moderate to low average permeabilities (Fig. 20). Most of the wells have maximum permeabilities less than 75 md and average permeabilities of a few tens of md. Anomalously high or low permeabilities are restricted to small areas having elongate shapes oriented parallel to the inferred direction of depositional strike. Compared to most measured values, the K-8 reservoir in the State Tract 49-2 well (Fig. 11) has abnormally high maximum (605 md) and

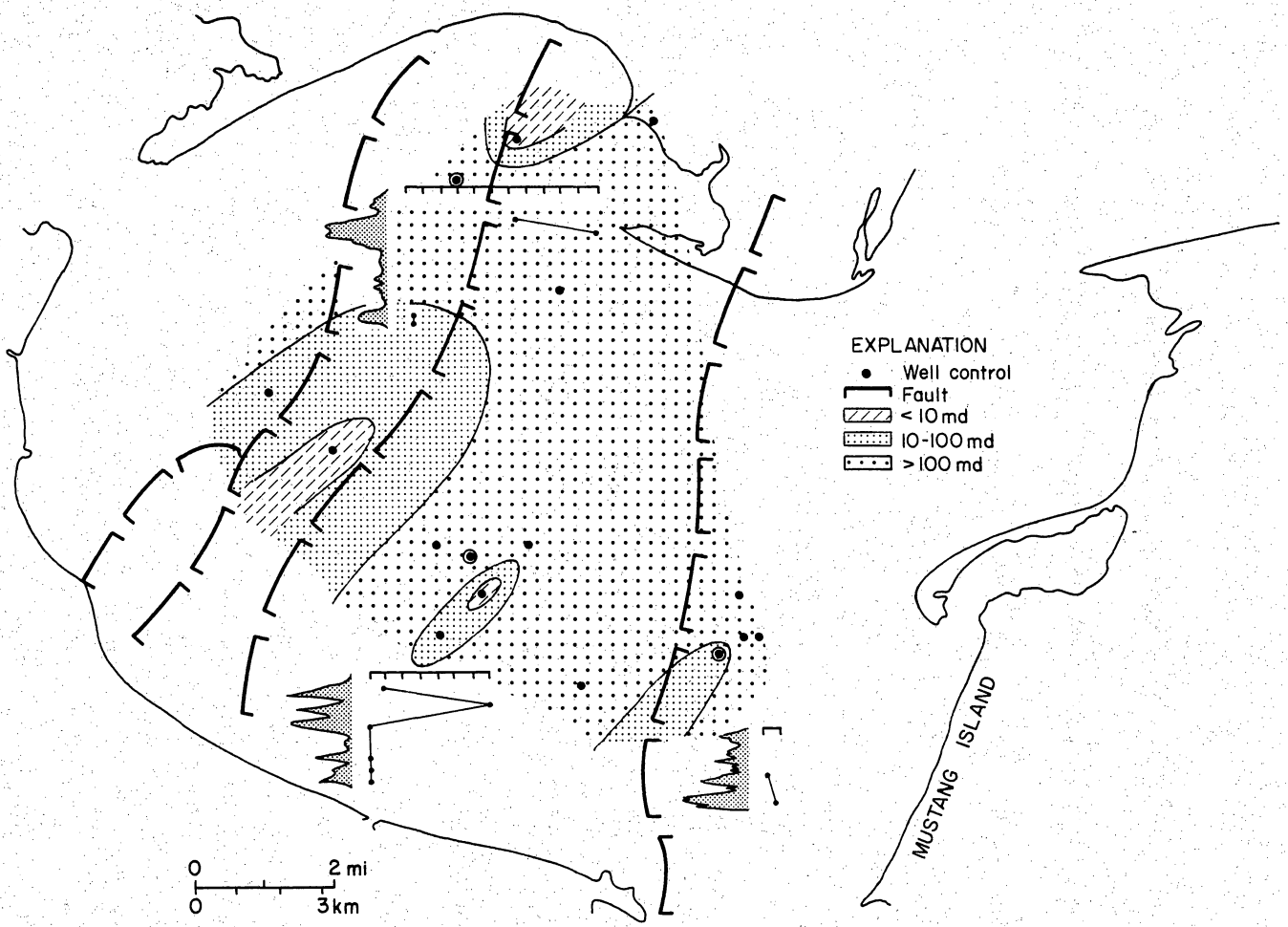

Figure 19. Spatial variations in average permeability for the J-3 shelf sandstone and siltstone reservoir. Spontaneous potential patterns and vertical permeability profiles are for circled wells. Permeability scale graduated in hundreds of millidarcies.

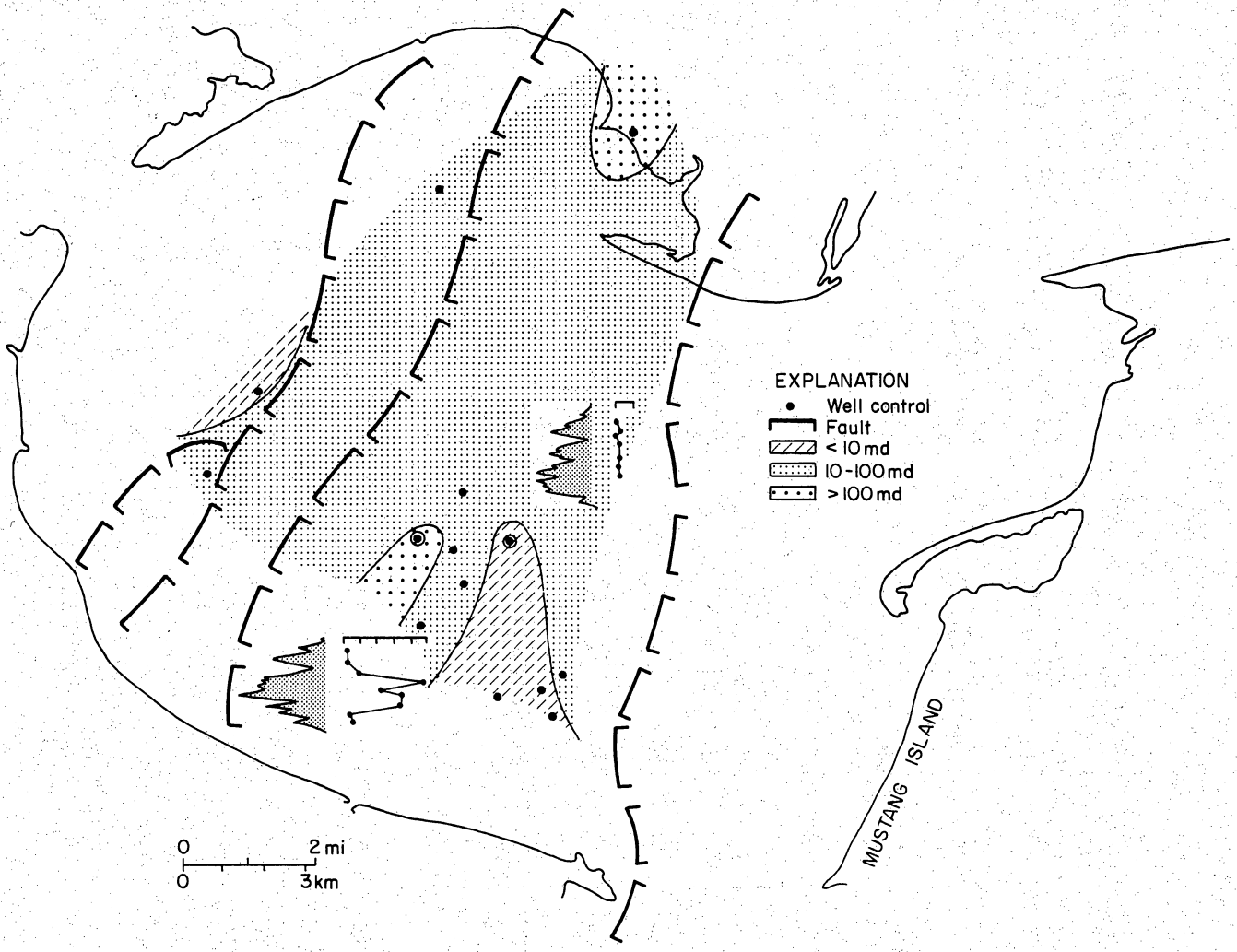

Figure 20. Spatial variations in average permeability for the K-8 distal shoreface and inner shelf sandstone reservoir. Spontaneous potential patterns and vertical permeability profiles are for circled wells. Permeability scale graduated in hundreds of millidarcies.

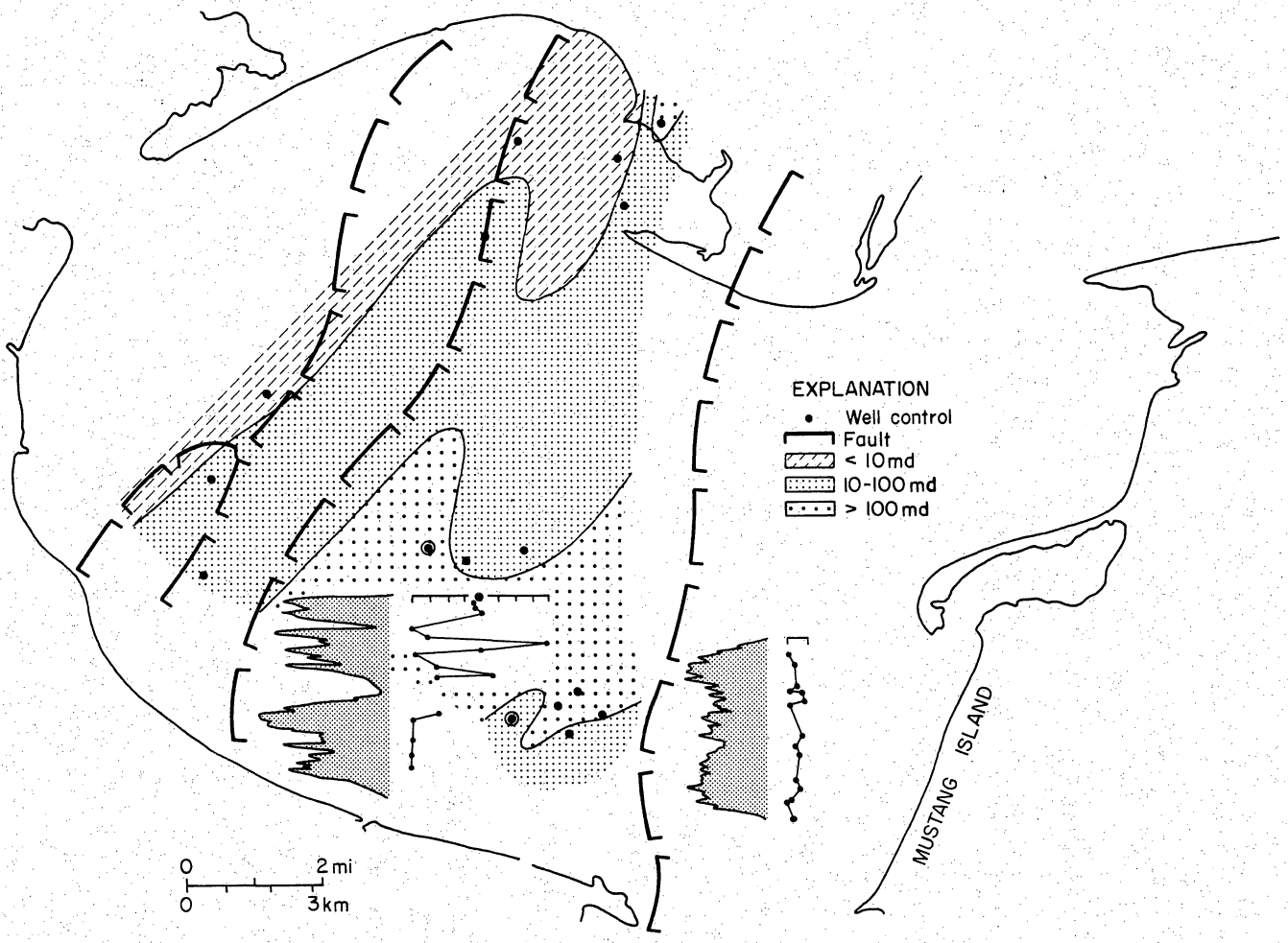

Figure 21. Spatial variations in average permeability for the L-2 distal shoreface and inner shelf sandstone reservoir. Spontaneous potential patterns and vertical permeability profiles are for circled wells. Permeability scale graduated in hundreds of millidarcies.

average (129 md) permeabilities.

The L-2 reservoir does not have a dominant class of average permeability, rather it exhibits a more systematic decrease in average permeability both landward and seaward from a central zone of highest average permeability (Fig. 21). Maximum values of 200 to 300 md are typical of the most permeable zones whereas maximum values of less than 50 md are typical of the zones of intermediate permeabilities. Like most other reservoirs in the State Tract 49-2 well, the L-2 reservoir (Fig. 12) has abnormally high maximum (866 md) and average (310 md) permeabilities.

The areas of higher and lower permeabilities (Figs. 19, 20, and 21) occur in bands that are spaced a few kilometers apart and are oriented subparallel to depositional strike. This repetitive pattern strongly suggests that alongshelf storm-generated currents selectively sorted the sand sheets causing some zones to be more mobile than others. Migrating low-relief bedforms within the mobile zones would have been preferential sites for the accumulation of relatively thick beds dominated by physical structures. Rapid deposition and thickness of these beds would have minimized burrowing by the benthic fauna, thereby promoting preservation of moderately high permeabilities.

Shore-parallel zones of preferential sorting and sediment transport produced by strong geostrophic bottom currents during storms have been documented for the modern Texas shelf (Morton in press). The elongate geometries, alongshelf orientations, and cross-shelf spacings of these modern features are similar to those observed in the Frio sediments (Figs. 19, 20, and 21), which suggests a common origin. The modern storm features formed about 16 km (10 mi) from the shoreline and in water depths of about 18 m (60 ft), which is a setting similar to that envisioned for deposition of the Frio shelf sandstones (Fig. 17). Preservation of the Frio storm beds was enhanced by high rates of sedimentation, rapid subsidence, and the high frequency of combined wave and current flow that transported sand onto the normally muddy shelf.

Reservoir quality of the principal sandstone facies can be compared by integrating electric-log patterns with sedimentological attributes and pore properties taken from core descriptions and laboratory measurements. Such a comparison reveals that the best reservoir quality occurs in the slightly coarser-grained sandstones where physical structures are preserved and where late-stage calcite cement is patchy or sparse. Conversely, reservoir quality is poor where pervasive calcite cementation and intensive bioturbation have created internal heterogeneities that disrupt fluid flow.

The previously described stacking and amalgamation of storm beds causes a high degree of variability in the vertical arrangement of porosity and permeability trends. Despite the apparent lack of order and near randomness to the thickness and quality of these units, there are some general associations that can be quantified from the available cores. The most common associations of pore properties in decreasing order of reservoir quality are: high porosity and high permeability, moderate to high porosity and intermediate permability, moderate porosity and variable permeability, moderate porosity and impermeable, and low porosity and impermeable.

Inner shelf and distal shoreface sequences are thin-bedded amalgamations composed of siltstone and very fine sandstone alternating with thin mudstone interbeds. The siltstone and sandstone beds generally have moderately good porosity but extremely low permeability (no measureable permeability or tens of millidarcies) because the physical structures have been obliterated by thorough bioturbation. Exceptions to these generalizations can occur where the primary sedimentary structures are preserved and secondary porosity is extensively developed in the non-burrowed intervals. The alternating thin beds with highly variable permeabilities generally make these heterogeneous sandstones poor oil reservoirs with low recovery efficiencies; however, they make moderately good gas reservoirs because of the higher relative permeabilities to gas.

In contrast to the shelf mudstones and sandstones, the nearshore sandstone facies (upper shoreface and beach environments) are thick, relatively homogeneous fine-grained sandstone sequences having slightly coarser textures (they contain less silt) and slightly better sorting. The physical sedimentary structures in these shoreface sandstone units are horizontal to slightly inclined parallel laminations with some ripple laminations. The structures are usually well preserved and burrowing is only a minor feature that is usually restricted to thin isolated intervals. As a result, the reservoirs associated with these facies contain thick beds with relatively high porosities and high permeabilities (hundreds of millidarcies) that act as single hydrologic subdivisions. The nearshore sandstone facies exhibit exceptionally good reservoir quality because of these highly porous and permeable zones. Consequently, some of the most prolific and efficient oil and gas reservoirs with strong water drives are associated with these lower Frio sandstones.

During deposition of the lower Frio sandstones, minor changes in rates of sedimentation or subsidence caused relative changes in shoreline position and water depth that resulted in the aggradation of nearshore sediments. The repetitive stacking of slightly more distal and proximal storm beds produced some pore property associations that are nearly opposite to those predicted using the

general observations described above. The most obvious differences are seen in the intrawell nonuniformities for reservoirs occurring below the top of geopressure. For example, thin beds such as the J-3 reservoir (Fig. 19), can have average permeabilities that are much higher than those of more proximal shoreface deposits, such as the L-2 reservoir (Fig. 21). The basinward increase in average permeability for the L-2 reservoir is also opposite to the trend that would be expected using conventional reservoir models. These observations, as well as others for low-permeability barrier-core reservoirs (I-4 overlying the J-3) suggest that the thin impermeable zones retard water circulation and limit water-rock interaction in the most permeable zones, thus preserving vestiges of original pore properties. In contrast, thick zones of originally permeable sandstone allow extensive circulation and precipitation of authigenic cements, thus reducing the extant reservoir quality.

Hydrocarbon Composition

Frio sandstone reservoirs of shallow marine origin have produced more than 232 bcf of gas in the Encinal Channel (143 bcf), Corpus Channel (49 bcf) and West Mustang Island (38 bcf) fields (International Oil Scouts 1985). The most prolific reservoirs, such as the K-2, K-3, K-8, and M-4 reservoirs, have each produced between 20 and 40 bcf of gas as well as minor amounts of condensate and oil. The structural traps containing the hydrocarbons are faulted anticlinal closures and dip reversals associated with large-scale rollover into major listric faults.

Organic geochemical analyses from the Portland field (location shown in Fig. 3) confirm that Frio sediments are poor source rocks because of their thermal immaturity and low concentrations of organic matter suitable for the generation of hydrocarbons (Galloway et al. 1982). Most shale samples contain less than 0.3 percent total organic carbon and the organic matter is mainly of terrestrial origin, although there is a systematic increase in marine kerogen below 2,400 m (8,000 ft) (Dow 1981) where the shallow-marine sandstone and mudstone facies predominate. In general, the types of kerogen present in these Frio sediments would yield small amounts of mostly dry gas. Like most of the major Frio reservoirs, the barrier and shelf sandstones occur above the depth of hydrocarbon generation, which is estimated at 3,400 m (11,150 ft) in the Corpus Christi Bay area (Dow 1981). The fact that these very low yield rocks contain abundant gas with some liquids indicates that the hydrocarbons originated deeper in the basin and migrated into the shorezone and shelf sandstones.

Formation Properties and Fluid Flow

Numerous in situ measurements taken from shelf sandstone reservoirs of the Frio Formation were used to analyze probable paths of fluid movement from deep within the basin (Figs. 22 and 23). Because of the interdeltaic setting, Gulfward dip, and down-to-the-basin growth faults in the area, younger sediments have greater shale content in a basinward direction at uniform depths of between 2,700 and 3,300 m (9,000 and 11,000 ft) (Fig. 23). The Frio shorezone sandstones grade downward and basinward into shelf sandstones that are interbedded with marine shale. Formation temperatures and pressure gradients also generally increase downward accompanying the decrease in sandstone percent and the stratigraphic displacement across major expansion faults. Abrupt increases in thermal gradient and pressure gradient, occurring at depths of about 3,000 m (10,000 ft), mark the thin transition zone that separates the hydropressured and geopressured hydrodynamic regimes (Morton and Land 1987).

Mapped formation properties at a uniform depth of 2,700 m (9,000 ft) (Fig. 22) clearly illustrate the subregional variations that are attributed to differential fluid movement along the fault planes and through the porous sediments. Near the Encinal Channel field, equilibrium formation temperatures and total dissolved solids (TDS) of formation water attain maximum values. This area of slightly elevated temperatures and concentrated brines occurs where the maximum thickness of Frio

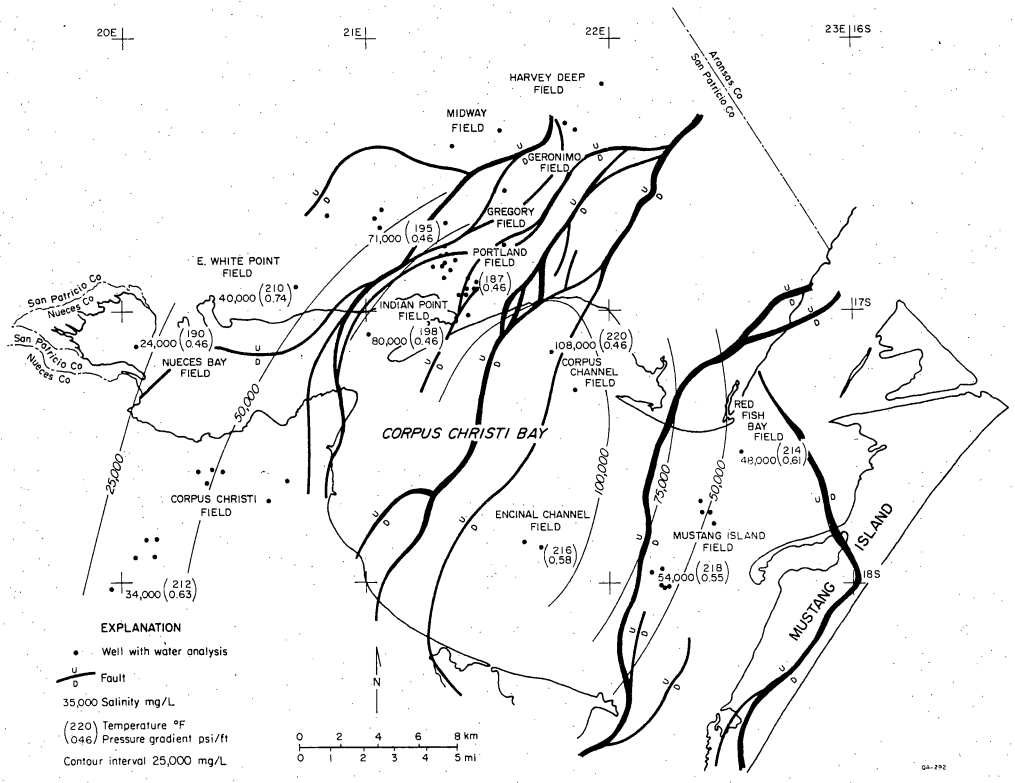

Figure 22. Average measured formation properties at 2,700 m (9,000 ft) for fields producing in and around Corpus Christi Bay. From Morton et al. (1980).

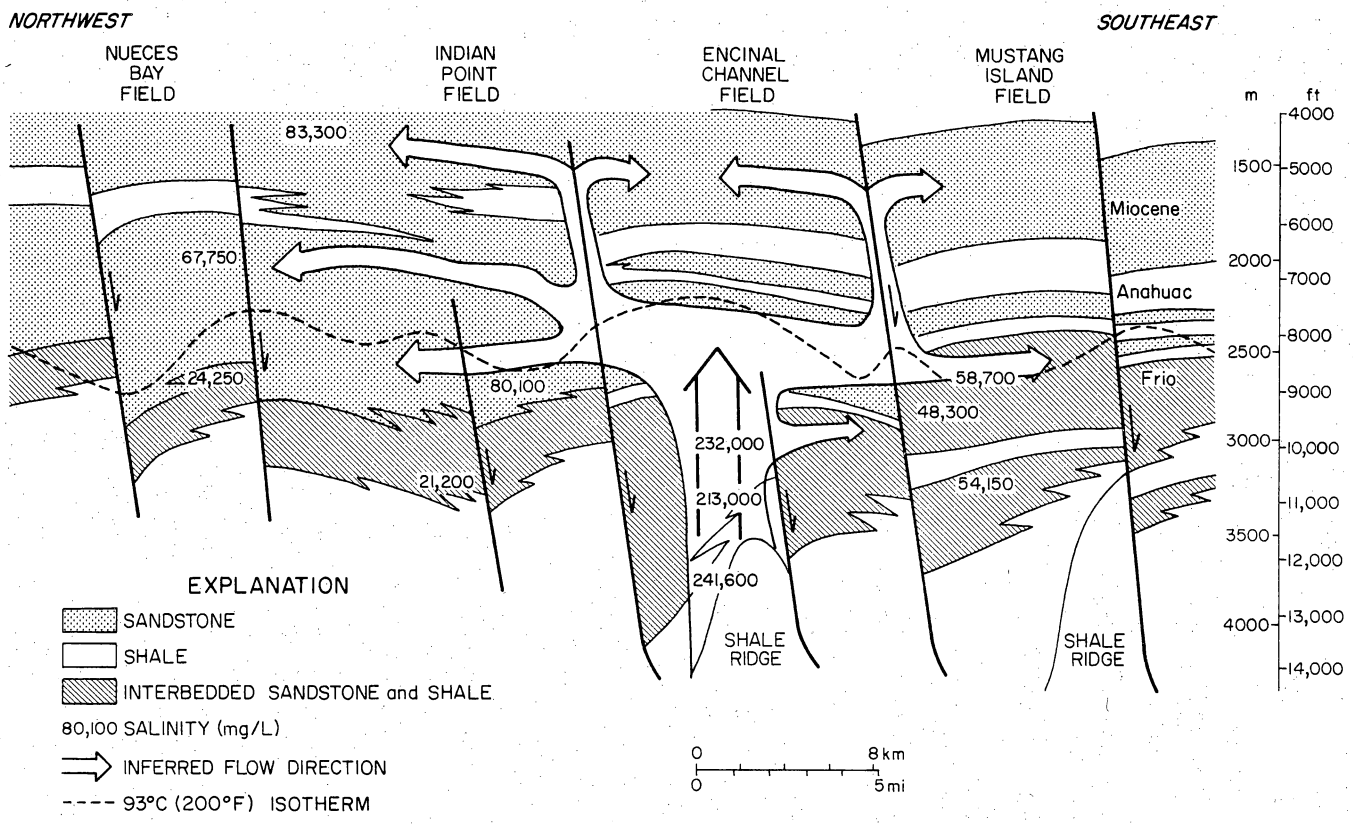

Figure 23. Generalized structural and stratigraphic framework of Tertiary sediments in the Corpus Christi area showing interpreted pathways of fluid migration and zones of brine mixing. Field locations shown on figure 22.

sandstones is at its basinward limit. The salinity maximum also overlies several shale diapirs (Fig. 23) formed by the emplacement of Vicksburg shales into overlying lower Frio sediments (Bishop 1977). Salinities are considerably lower and interstitial pressure gradients are slightly higher in surrounding sediments at comparable depths. The normal occurrence of low-salinity formation water in the shale-rich sediments of this hydrochemical subregion is probably related to physical compaction and thermal conversion of smectite to illite (Morton and Land 1987).

The variations in formation temperature, pore pressure, and formation-water salinity indicate that hot, highly concentrated brines ascended along the shale diapir structural trend and mixed with low salinity resident water in the adjacent interval of interbedded sandstone and shale. Most of the sediments peripheral to the area of upwelling and below 3,000 m (10,000 ft) contain diluted formation water and apparently were not intruded by the plume of ascending brines that probably originated in the deeply buried Mesozoic section of the basin. Waters in the overlying massive sandstone section have TDS concentrations greater than seawater, suggesting a mixture of original pore water and upwelling brines. The greater hydraulic conductivity of the thick, highly permeable sandstones allowed extensive fluid movement and lateral migration of the invading water masses. The slightly lower pressure gradients in the area of inferred upwelling may signify the reduced pore pressures that accompanied fluid flow. Together the slightly higher temperatures, lower pressure gradients, and higher salinities may indicate the preferred paths of lateral intrusion through permeable beds and vertical migration along regional faults (Fig. 23).

Additional evidence corroborating the idea of local fluid expulsion is provided by the volume of hydrocarbons produced from each of the three fields near the interpreted plume. Assuming that cumulative production of mature fields is an indicator of total in-place reserves, then the Encinal Channel field is three and four times larger than the Corpus Channel and West Mustang Island fields respectively. This pattern of decreasing hydrocarbon volume away from the plume center agrees with the proportional distribution predicted by the fluid flow model.

ACKNOWLEDGMENTS

Portions of this study were funded by grants from Standard Oil Production Company and the U. S. Department of Interior, Minerals Management Service under MMS Agreement No. 14-12-0001-30316. We thank the anonymous reviewers who improved the manuscript by making helpful suggestions. Our appreciation is extended to all who contributed to the preparation of the manuscript and especially to James Miller who provided the point-count data.

Aigner, T., 1985, Storm depositional systems: Lecture Notes in Earth Sciences No. 3, Heidelberg, Springer-Verlag, 174 p.

Berg, R. R., and Powell, R. R., 1976, Density-flow origin for Frio reservoir sandstones, Nine Mile Point field, Aransas County, Texas: Gulf Coast Association of Geological Societies Transactions, v. 26, p. 310-319.

Bishop, R. S., 1977, Shale diapir emplacement in South Texas, Laward and Sheriff examples: Gulf Coast Association of Geological Societies Transactions, v. 27, p. 20-31.

Dow, W. G., 1981, Geochemical analysis of selected samples from the Kelley Bell No. D-1 well, San Patricio Co., Texas: Robertson Research Inc., report to the Bureau of Economic Geology, unpaginated.

Galloway, W. E., 1986a, Reservoir facies architecture of microtidal barrier systems: Am. Assoc. Petroleum Geologists Bull., v. 70, p. 787-808.

Galloway, W. E., 1986b, Depositional and structural framework of the distal Frio Formation, Texas coastal zone and shelf: The University of Texas at Austin, Bureau of Economic Geology Geological Circular 86-8, 16 p.

Galloway, W. E., Hobday, D. K., and Magara, K., 1982, Frio Formation of the Texas Gulf Coast Basin- depositional systems, structural framework, and hydrocarbon origin, migration, distribution, and exploration potential: The University of Texas at Austin, Bureau of Economic Geology Report of Investigations No. 122, 78 p.

Hayes, M. O., 1967, Hurricanes as geological agents; case studies of hurricane Carla, 1961, and Cindy, 1963: The University of Texas at Austin, Bureau of Economic Geology Report of Investigations No. 61, 56 p.

International Oil Scouts Association, 1985, International oil and gas development: Austin, Texas, v. 51 and 52, part II, production, 794 p.

Jackson, M. P. A., and Galloway, W. E., 1984, Structural and depositional styles of Gulf Coast Tertiary continental margins: applications to hydrocarbon exploration: Am. Assoc. Petroleum Geologists Course Note Series No. 25, 226 p.

Loucks, R. G., Dodge, M. M., and Galloway, W. E., 1986, Factors controlling porosity and permeability of hydrocarbon reservoirs in lower Tertiary sandstones along the Texas Gulf coast: The University of Texas at Austin, Bureau of Economic Geology Report of Investigations No. 149, 78 p.

McCave, I. N., 1985, Recent shelf clastic sediments, *in* Brenchley, P. J., and Williams, B. P. J., eds., Sedimentology, recent developments and applied aspects: Geological Society of London, Special Publication, p. 49-65.

McGowen, J. H., and Morton, R. A., 1979, Sediment distribution, bathymetry, faults, and salt diapirs, submerged lands of Texas: The University of Texas at Austin, Bureau of Economic

Geology Special Publication, 31p.

Morton, R. A., 1981, Formation of storm deposits by wind-forced currents in the Gulf of Mexico and North Sea: International Asssociation of Sedimentologists, Special Publication 5, p. 385-396.

Morton, R. A., Ewing, T. E., and Tyler, N., 1980, Consolidation of geopressured geothermal studies: The University of Texas at Austin, Bureau of Economic Geology report to the Department of Energy, contract no. DE-AC08-79ET27111, 195 p.

Morton, R. A., and Land, L. S., 1987, Variations in formation water chemistry, Frio Formation (Oligocene), Texas Gulf Coast: Am. Assoc. Petroleum Geologists Bull., v. 71 , p. 191-206.

Morton, R. A., in press, Nearshore responses to great storms, *in* Clifton, H. E., ed., Sedimentologic consequences of convulsive geologic events: Geological Society of America Special Publication.

Parker, G., 1982, Conditions for the ignition of catastrophically erosive turbidity currents: Marine Geology, v. 46, p. 307-327.

Seilacher, A. 1978, Use of trace fossils for recognizing depositional environments, *in* Basan, P. B. ed., Trace fossil concepts: Soc. Econ. Paleontologists and Mineralogists Short Course No. 5, p. 167-181.

Swift, D. J. P., Han, G., and Vincent, C. E., 1986a, Fluid processes and sea-floor response on a modern storm-dominated shelf: middle Atlantic shelf of North America. Part I: the storm-current regime, *in* Knight, R. J., and McLean, J. R., eds., Shelf sands and sandstones: Canadian Society of Petroleum Geologists Memoir 11, p. 191-211.

Swift, D. J. P., Thorne, J. A., and Oertel, G. F., 1986b, Fluid processes and sea-floor response on a modern storm-dominated shelf: middle Atlantic shelf of North America. Part II: response of the shelf floor, *in* Knight, R. J., and McLean, J. R., eds., Shelf sands and sandstones: Canadian Society of Petroleum Geologists Memoir 11, p. 99-119.

Wilkinson, B. H., 1975, Matagorda Island, Texas: the evolution of a Gulf Coast barrier complex: Geol. Soc. America Bull., v. 86, p. 959-967.

Winker, C. D., 1982, Cenozoic shelf margins, northwestern Gulf of Mexico Basin: Gulf Coast Association of Geological Societies Transactions, v. 32, p. 427-448.

Wright, L. D., Boon, J. D., Green, M. O., and List, J. H., 1986, Response of the mid shoreface of the southern mid-Atlantic to a "northeaster": Geo-Marine Letters, v. 6, p. 153-160.

Zeller, E. J., 1964, Cycles and psychology: Kansas Geological Survey Bulletin No. 169, p. 631-636.